Title: Ultraviolet radiation accelerates photodegradation under controlled conditions but slows the decomposition of senescent leaves from forest stands in southern Finland

Authors: Marta Pieristè[1,2*], Santa Neimane[1,3,4*], Twinkle Solanki[1], Line Nybakken[5], Alan G. Jones[6], Estelle Forey[2], Matthieu Chauvat[2], Jevgenija Ņečajeva[3], T. Matthew Robson[1✉]

Authors' Institutions:

[1✉]Organismal and Evolutionary Biology (OEB), Viikki Plant Science Centre (ViPS), Faculty of Biological and Environmental Science, P.O. Box 65, 00014, University of Helsinki, Finland.

[2]Normandie Université, UNIROUEN, Ecodiv URA/EA1293, IRSTEA, FR Scale CNRS 3730, Rouen, France

[3]Department of Plant Physiology, University of Latvia, Jelgavas street 1, LV-1004, Riga, Latvia.

[4]Latvian State Forest Research Institute (Silava), Rīgas iela 111, Salaspils, Salaspils pilsēta, LV-2169, Latvia.

[5]Faculty of Environmental Sciences and Natural Resource Management, CERAD, Norwegian University of Life Sciences, 1432 Ås, Norway.

[6]Forest Systems, Scion. 49 Sala Street, Private Bag 3020, Rotorua 3046, New Zealand.

*Joint first author contribution

Corresponding Author: T. Matthew Robson[1] matthew.robson@helsinki.fi

Accepted in : *Plant Physiology and Biochemistry*.

Article reference number: **PLAPHY5920**

Abstract

Depending on the environment, sunlight can positively or negatively affect litter decomposition, through the ensemble of direct and indirect processes constituting photodegradation. Which of these processes predominate depends on the ecosystem studied and on the spectral composition of sunlight received. To examine the relevance of photodegradation for litter decomposition in forest understoreys, we filtered ultraviolet radiation (UV) and blue light from leaves of *Fagus sylvatica* and *Betula pendula* at two different stages of senescence in both a controlled-environment experiment and outdoors in four different forest stands (*Picea abies, Fagus sylvatica, Acer platanoides, Betula pendula*). Controlling for leaf orientation and initial differences in leaf chlorophyll and flavonol concentrations; we measured mass loss at the end of each experiment and characterised the phenolic profile of the leaf litter following photodegradation. In most forest stands, less mass was lost from decomposing leaves that received solar UV radiation compared with those under UV-attenuating filters, while in the controlled environment UV-A radiation either slightly accelerated or had no significant effect on photodegradation, according to species identity. Only a few individual phenolic compounds were affected by our different filter treatments, but photodegradation did affect the phenolic profile. We can conclude that photodegradation has a small stand- and species- specific effect on the decomposition of surface leaf litter in forest understoreys during the winter following leaf fall in southern Finland. Photodegradation was wavelength-dependent and modulated by the canopy species filtering sunlight and likely creating different combinations of spectral composition, moisture, temperature and snowpack characteristics.

Keywords
Photodegradation; phenolic compounds; UV radiation; flavonoids; understorey light environment.

Abbreviations

UV: ultraviolet radiation

PAR: Photosynthetically Active Radiation

FW: Fresh weight

DW: Dry weight

C: carbon

N: nitrogen

C:N: Carbon to nitrogen ratio

[C]: Concentration of Carbon

[N]: Concentration of Nitrogen

Lig:N: Lignin to nitrogen ratio

LAI: Leaf Area Index

GLI: Global Light Index

HPLC: High-performance liquid chromatography

MeOH: Methanol

Introduction

Decomposition is a key ecological process in nutrient cycling, during which organic compounds are broken down and thus become available for primary producers. In temperate and boreal forests, decomposition is controlled by many biotic and abiotic factors, such as temperature, moisture, frost, freeze-thaw cycles, soil pH, sunlight, microbial communities, soil fauna and fertility, etc. [1-6]. Litter traits, together with climatic variables, explain up to 70% of the decomposition rates in terrestrial ecosystems on a global scale [7]. However, at a continental scale, the rate of decomposition is mainly controlled by litter chemistry [8]. Moreover, canopy trees may impact decomposition directly through their leaf litter traits or indirectly by altering the microenvironment including solar radiation in the understorey; this effect at the local level may have a bigger impact on decomposition than large-scale climatic gradients [9].

Solar radiation impacts decomposition, both directly and indirectly - through photochemical mineralization, photopriming, and microbial photoinhibition [10], together these processes are known as photodegradation. In arid and semi-arid environments, photodegradation has been shown to play a key role in the control of litter decomposition rate and to be effected by UV radiation and the short-wavelength region of the visible spectrum (such as blue and green light) [11, 12]. However, worldwide studies have presented conflicting results regarding factors that enhance the photodegradation of plant litter [13, 14]. The variability of climatic conditions (cloud cover, rainfall, Ozone Layer thickness, pollutants concentration, etc.), impacting the total amount of incoming radiation, makes it hard to assess the role of photodegradation in global nutrient fluxes and how they might respond to climate change [15-18]. At mid-high latitudes, large seasonal differences in sunlight hours mean that, when overstorey canopies are open and there is no snow cover during the autumn and early spring,

high solar irradiances can transiently reach the understorey. Nevertheless, the total irradiance received annually at the forest floor is still quite small compared with areas with no canopy cover [19].

While solar UV radiation can on balance enhance the rate of decomposition [20], its positive and negative effects may even out because UV-B and UV-A radiation differ in their effect on decomposition according to environmental conditions and litter chemistry [12]. Typically, traits associated with litter chemistry such as its concentration of lignin and phenolics (such as tannins), carbon to nitrogen ratio (C:N), lignin to nitrogen ratio (lig:N), etc., were thought to determine the rate of decomposition [21]. However, recent studies have found traditional indices of litter quality to poorly explain litter mass loss due to photodegradation in arid environments [22, 23].

The morphology and biochemistry of living leaves determine their optical properties, but once senescent the continued capacity of these leaf traits to interact with sunlight, and potentially influence photodegradation, has not been widely studied. Some of the phenolic compounds in the leaf epidermis, absorb UV radiation and consequently screen the interior of the leaf potentially interfering with photodegradation [24]. During leaf senescence, when plants remobilise the nutrients held in chlorophyll, the content of epidermal UV-screening phenolics is also known to change [25, 26]. Green leaves are rich in chlorophyll and photosynthetic enzymes which have a high nitrogen content, making them more palatable to decomposers and faster to decompose [27] than yellow leaves.

To test how spectral composition affects photodegradation and identify its role in the initial phase of leaf litter decomposition in forest understoreys, we performed two parallel experiments using filters to create different light treatments. We tested the effect of the blue

88 and UV portions of the spectrum on photodegradation of senescent leaves (1) in a controlled
89 experiment in a growth room, and (2) whether these effects remained evident in equivalent
90 leaves under the same set of filters in a decomposition experiment in forest stands. We
91 employed senescent leaves from two species with contrasting leaf morphological traits;
92 *Betula pendula* which is light-demanding and produces leaves with an exploitative strategy,
93 and *Fagus sylvatica* which grows in shadier stands and produces leaves with a conservative
94 strategy expected to be more recalcitrant. We deployed these leaves in adjacent forest stands
95 dominated by different canopy species designed to create continuum of understorey shade
96 (from dark to light stands - *Picea abies, Fagus sylvatica, Acer platanoides, Betula pendula*). In
97 order to test whether differences in pigment contents affecting leaf optical properties can
98 affect photodegradation, we employed leaf litter at two different stages of senescence (green
99 and yellow leaves). We expected green leaves to both photodegrade and decompose faster
100 than yellow leaves because they contain more labile compounds. We also placed leaves
101 under our filters in two different orientations (adaxial leaf epidermis facing upwards or
102 downwards): while leaf orientation has no ecological significance in itself, the penetration of
103 UV radiation through the adaxial and abaxial epidermis differs due to UV-screening by
104 epidermal flavonols. Moreover, the abaxial side of the leaf is richer in stomata which favour
105 light penetration [28]. Hence, leaf orientation will affect UV penetration into the leaf and
106 may serve as a control for exposure of the targets of photodegradation in the mesophyll to
107 UV radiation in otherwise similar leaves. We expected mass lost from decomposing leaves to
108 be affected by the spectrum of radiation received during photodegradation, with greater
109 mass loss from leaves exposed to UV radiation than those under dark or partially-attenuated
110 spectra. We hypothesize that leaves with the abaxial epidermis facing upwards would
111 decompose faster than leaves with the adaxial epidermis facing upwards, since the higher

112 phenolic content of the adaxial epidermis provides more effective screening of the mesophyll
113 from UV-radiation; and that this interaction between filter treatments and epidermal
114 phenolics would be visible in the phenolic profile of litter following photodegradation.

115 **Materials and Methods**

116 ***Sampling and preparation of leaves for controlled and forest experiments***

117 Leaves were harvested from six-year-old stands of *Betula pendula* and *Fagus sylvatica*,
118 planted in Viikki experimental plots at the University of Helsinki in southern Finland
119 (60°13'39.7'N, 25°01'09.5'E). This vegetation zone is where the hemi-boreal borders the
120 southern boreal region [29].

121 Leaves that received full sun in the canopy ("sun leaves") of approximately the same size (*c*
122 20 cm^2) were harvested in a systematic fashion, directly from the south-side and upper third
123 of each tree, avoiding the leaves at the tip of the branch and those closest to the trunk. Only
124 leaves with no visible signs of herbivory or pathogens were collected and not more than four
125 leaves per tree. Green leaves of *B. pendula* and *F. sylvatica* were harvested on 29-09-2016
126 during autumn leaf senescence; fully senescent yellow leaves of the same size and at the same
127 location on the trees as the green leaves, were harvested 8-14 days later.

128 Directly after leaf collection the petiole was removed, leaves were numbered and put into
129 plastic bags to restrict moisture loss and keep them fresh. Within 1 h of collection, the leaves
130 were scanned for leaf area, which was calculated using imageJ [30] following the protocol
131 from [31]. Leaves were then immediately weighed for fresh weight (FW) and optical
132 measurements of leaf pigments taken with a Dualex Scientific$^+$ device (Force-A, Paris, France)
133 on both sides of the leaves. These measurements give an index of epidermal flavonol content
134 and leaf chlorophyll contents based on chlorophyll fluorescence and absorbance at various

wavelengths of the spectrum, described by [32] and [33]. Since some chlorophyll is required as a reference for the flavonol and anthocyanin measurements, those values where chlorophyll was very low (Dualex Index < 3.0) were not considered reliable and were removed from the analyses. The same place on the lamina of all leaves was measured, two-thirds down from the tip to the side of the midrib.

For the experiment in controlled conditions, for maximum realism in leaf traits and microbial communities, fresh leaves were deployed immediately after their harvest, whereas oven dried leaves were used for the field experiment as it was impractical to install the two experiments simultaneously. For this field experiment, 576 leaves were dried at 37°C until they achieved a constant weight, which took 3 days for yellow leaves and 7 days for green leaves. Following the measurement of their dry mass, leaf area was remeasured and Dualex Scientific^{+} measurements repeated as mentioned above, to test whether the epidermal flavonol values for both sides of the leaf, as well as leaf chlorophyll content, were affected by drying (the relationships between these values for fresh and dried leaves are given in Fig. S1).

The very tight relationship between the FW and dry weight (DW) for green and yellow leaves of each species was used to obtain a conversion factor for calculations of mass loss involving fresh leaves used in the controlled experiment (Fig. S2).

Filter treatments attenuating light and UV radiation

In the controlled and forest experiments, four different plastic films were used to create the different filter treatments. These were: a solid black/white polyester (0.07 mm thick, Siemenliike Siren, Helsinki, Finland) attenuating the full spectrum ("Dark"); transparent polyethene (0.05 mm thick, 04 PE-LD; Etola, Jyväskylä, Finland) transmitting >95% of radiation throughout the spectrum ("Full-Spectrum"); Rosco #226 (0.2 mm thick, Supergel; Foiltek Oy,

158 Vantaa, Finland) attenuating UV-A and UV-B radiation ("No-UVA" in controlled experiment
159 and "No-UV" in field experiment), and Rosco #312 Canary Yellow (0.2 mm thick, Supergel;
160 Foiltek Oy, Vantaa, Finland) attenuating UV-A and UV-B radiation and blue light ("No-
161 UV/Blue"). Each filter was cut into 8-×-8-cm squares and attached to a leaf by a staple through
162 the base of the midrib and to a Teflon mosquito net (mesh size 1.5 mm). Half of the leaves
163 were arranged with their adaxial epidermis facing upwards and the other half with the abaxial
164 epidermis facing upwards, in 16 randomised complete blocks in the controlled environment
165 (Fig. S3A, B). A similar arrangement with 16 blocks per stand was employed in the forest
166 stands (Fig. S3C, D). The spectral transmittance of all filter materials was found not to differ
167 between before and after a period of exposure in the field exceeding the duration of the
168 experiments (data from Qing-Wei Wang - not shown).

169 ***Controlled Photodegradation Experiment***

170 The controlled experiment tested the effects of photodegradation on senescent leaves with
171 and without UV-A radiation and blue light under a broad LED spectrum (Fig. 1) containing
172 those spectral regions present in a forest understorey [34, 35]. A total of 256 fresh leaves
173 were divided among the treatments: 2 species × 2 leaf colours × 4 filter types × 16 replicate
174 leaves with either the adaxial or abaxial side facing upwards. Leaves were positioned on
175 mosquito netting on a metal shelf 40 cm beneath the light sources: UV-A LEDs (Z1-00UV00
176 365 nm GEN2 emittor, LED Engin, San Jose, CA, USA, 15 µmol m^{-2} s^{-1}) and broad-spectrum
177 visible LED light (AP67, Valoya, Helsinki, Finland). Leaves received 168 µmol m^{-2} s^{-1} (6.04 mol
178 m^{-2} d^{-1}) of photosynthetically active radiation (400-750 nm, PAR) plus 32 µmol m^{-2} s^{-1} (1.15
179 mol m^{-2} d^{-1}) of far red radiation; a similar exposure to those in the forest understoreys
180 between October and February (Fig. S4). The lamps were illuminated in a cycle on for 10
181 hours from 08:00-18:00 and off for 14 hours. The irradiance under each lamp treatment and

filter combination was measured with a Maya 2000 Pro array spectrometer (Ocean Optics Inc., Florida, USA), which had been calibrated for measurements of the UV-visible spectrum following [36] and [19] (Fig. 1). The temperature in the chamber was thermostatically controlled to 20°C day/ 18 °C night and monitored in each compartment with i-button sensors (Maxim Integrated, San Jose, United States) (Fig. S5). Leaf temperature was monitored with a micro-epsilon high-precision infra-red thermometer (Optris, Berlin, Germany) and was about 5°C above the ambient daytime temperature when illuminated (Fig. S6). These data showed that temperature was on average 0.8°C lower under the dark filter than the other filter treatments, and that the green *B. pendula* leaves were 1.0°C cooler than the other leaves on average, but otherwise there were no differences among leaves.

To account for any uncontrolled gradients in temperature and irradiance in the controlled environment, leaves were rotated under each set of lamps every 2 weeks throughout the experiment. After 6 weeks (44-50 days) of filter treatments the first half of the leaves were removed (average daily mass loss 0.540 %) and after 10 weeks (75-77 days) the remaining leaves were collected (average daily mass loss 0.534 %). The two harvest dates were normalised to mean daily relative mass loss as there was no significant different (or interaction with other factors) between the two harvested cohorts (data not shown).

Forest Decomposition Experiment

Senescing leaves were arranged in four different forest stands in Viikki, Helsinki (60°13'39.7'N, 25°01'09.5'E), as described above, on 07-10-2016 for *F. sylvatica* leaves and 19-10-2016 for *B. pendula* leaves, and collected on 11-04-2017 (6 months after the beginning of the experiment) for both species. The canopy trees in the four different stands of differing leaf area index (LAI) were 10-year-old *B. pendula* and 6-year-old *F. sylvatica*, and mature (>60

205 years old) *A. platanoides* and *P. abies* trees. Before starting the experiment, any ground
206 vegetation (minimal) was removed from directly under and surrounding the leaves, and a thin
207 litter layer consisting only of the surrounding leaf litter at each stand was placed between the
208 ground and the mosquito net holding the leaves and filters to ensure conditions were natural
209 and homogeneous (Fig. S2C, D). The mosquito net was anchored to the ground using nails. A
210 fine bird net, minimally affecting the irradiance received by the experiment, was placed like a
211 wigwam over the leaves to deflect any falling or blown leaves, which might otherwise build-
212 up on the filters obscuring the sunlight. Any leaves stuck on the net were cleaned away every
213 few days but any snow that was not intercepted by the canopy was allowed to accumulate
214 and melt naturally on the filters over winter.

215 The spectral irradiance was measured in all the forest stands using an array
216 spectroradiometer (Maya2000 Pro Ocean Optics, Dunedin, FL, USA; D7-H-SMA cosine
217 diffuser, Bentham Instruments Ltd, Reading, UK) that had been calibrated within the previous
218 12 months for measurements spanning the regions of solar UV radiation and PAR (see
219 Hartikainen et al 2018 for details of the calibration), [37, 38] (Table S1 and S2). Hemispherical
220 photos were taken at the same locations as spectral irradiance, to characterize canopy cover
221 by calculation of the global light index (GLI) and the leaf area index (LAI) with the software
222 Hemisfer [39, 40] following the protocol from Hartikainen et al 2018. Above-canopy PAR was
223 obtained from the Viikki Fields Weather Station of the University of Helsinki located within
224 the experimental site (60°13'39.7'N, 25°01'09.5'E). UV radiation was obtained from the
225 Finnish Meteorological Institute (FMI) weather station located in the adjacent suburb of
226 Kumpula (60°12'00.0"N, 24°57'36.0"E), Helsinki [41, 42]. Below-canopy irradiance was
227 modelled from above-canopy irradiance data, whereby GLI and LAI estimated from
228 hemispherical photos were used to model selective filtration by the different canopies,

validated against understorey spectroradiometer measurements following the protocol in [43].

Mass loss, HPLC and C:N Analyses of Leaf Litter

Following collection of the experimental leaf litter at the end of their decomposition and photodegradation periods, leaves were separated from their filters taking care not to lose any fragments of leaf. They were placed in paper bags and dried at 37°C in a ventilated desiccating oven until reaching a constant weight (after 13 days) to obtain their DW. Worm casts and dirt were carefully removed from leaves that had decomposed outdoors using a small paintbrush, in order to reduce the error due to contamination from inorganic particles.

Biochemical analyses were done on litter samples from the controlled environment. To prepare leaves for biochemical analyses, first the midrib was cut out of the leaf, as was the small mark on the lamina used to number the leaf prior to decomposition. The remaining leaf lamina material was placed into a 1.5-ml Eppendorf tube. To grind the leaf material, 25 glass beads of 1 mm diameter (#22.222.0005, Retsch GmbH, Haan, Germay) were added to each tube, and tubes were shaken for 1.5 to 2 minutes in a Silamat S6 mixer (Ivoclar Vivadent, Amherst, USA) at rotation speed of 4500 rpm. Dry powdered samples were stored in the dark at room temperature between grinding and analysis.

For the elemental analysis, 5-6 mg of ground leaf material was used. The total nitrogen (N) and carbon (C), and the C:N ratio per leaf dry-mass were determined using a Vario Micro Cube (Elemental Analysis Systems GmbH, Hanau, Germany). For the analysis of phenolic compounds by HPLC (high-performance liquid chromatography), 10 mg of leaf material was used. Leaf extraction and HPLC analysis was performed as in [44]. Compounds were identified by comparing the absorbance spectrum (270 - 320 nm) to commercially available

252 standards. Flavonoid glycosides were identified down to their respective aglycones, and
253 numbered (e.g. quercetin glyc1, quercetin glyc2) if we were not able to identify the type and
254 position of glycosylation.

255 The same samples run for the HPLC analysis were used two-days later to determine the
256 condensed tannin content by acid-butanol assay following the protocol of [45]. The content
257 of MeOH-insoluble condensed-tannin residues from phenolic compound extraction were
258 mixed with methanol to give a total sample volume of 0.5 ml. Afterwards 3 ml of butyric acid
259 (95% butanol, 5% hydrochloric acid) and 100 µl Fe reagent (2 M HCL with 2 % ferric
260 ammonium sulphate) were added and mixed. The sealed sample tubes were placed in boiling
261 water for 50 min and once cooled their absorbance at 550 nm was measured with an UV-
262 1800 spectrophotometer (Shimadzu Corp., Kyoto, Japan).

263 ***Data Analysis***

264 We first tested the effect of species (*Betula pendula* and *Fagus sylvatica*) and phase of
265 senescence (green and yellow coloured leaves) on the rate of mass loss and on the
266 biochemistry of leaf litter from the controlled experiments with a mixed-model ANOVA using
267 the function lmer from package lme4 (https://CRAN.R-project.org/package=nlme).

268 The effects of our different filter treatments (Dark, No-UVA/Blue, No-UVA, Full-Spectrum) and
269 leaf orientation were tested separately for each species and leaf colour, using a split-plot
270 mixed-model ANOVA. Filter treatment was the main fixed effect, while orientation (adaxial
271 or abaxial epidermis up) was the split-plot effect, and harvest cohort was a random factor.
272 Function glht from Multcomp package was used to obtain individual pair-wise comparisons,
273 and Holm's adjustment was applied between treatments to account for multiple
274 comparisons.

For the forest experiment, a three-way mixed model ANOVA was used, with stand an additional fixed effects factor in the models, otherwise the model was described above for mass loss in the controlled experiment. To better visualise the effects of filter treatments on mass loss and leaf chemistry in both experiments against a fixed baseline that is normalised for differences due to species and leaf colour, these data were plotted as response ratios for each filter type compared with the results under the dark filter.

When analysing HPLC data for birch leaves, because of insufficient leaf mass remaining from all levels of treatments at both leaf orientations, orientation could not be included as a fixed factor in the ANOVA model. As well as the ANOVA, patterns in the composition of the phenolic profile were mapped against explanatory variables for each species' litter by nonmetric multidimensional scaling using function metaMDS from community ecology package, vegan [46].

Relationships between abaxial and adaxial flavonols and anthocyanins, chlorophyll content and nitrogen balance index, as well as fresh weight and leaf area, were examined by determining correlation coefficients. Linear regression models were tested using R function lm. To plot non-linear relationships, i.e. between leaf nitrogen content and leaf carbon/nitrogen ratio, we used ggplot2 package [47] and package ggpmisc version 0.2.15 [48] fitting a GAM smoother (stat_smooth). Irradiance spectra measured with the Maya 2000 Pro spectrometer were pre-processed using the R packages Ooacquire and Photobiology [49]. All data were analysed in R core version 3.3.3 [50].

Results

Spectral irradiance in the Forest Experiment

The spectral irradiance differed among the forest stands (Fig. 1C and 1D, Fig. S4). The leaf litter in the *B. pendula* stand received the highest PAR and UV radiation over the study period (Table S3 Fig. S4) since this stand transmitted about 69% and 66% of above-canopy PAR and UV, respectively. The *Acer platanoides* stand transmitted 46% of above-canopy PAR, 51% of UV radiation and 52% of blue light, followed by the *Fagus sylvatica* stand (19% of PAR, 16% of UV, 13% blue) and the *Picea abies* stand (13% of PAR and UV, 14% blue: Fig. S4 and Table S3).

Effect of species, senescence stage and leaf orientation on harvested leaf traits.

The traits of sampled green and yellow leaves from *F. sylvatica* and *B. pendula* are given in table S4. In both species, epidermal flavonol content, as measured by Dualex, decreased during leaf senescence (from green to yellow leaves), in addition to the expected drop in chlorophyll and water contents (Table S4). Epidermal flavonols were higher for *B. pendula* than *F. sylvatica* leaves at the equivalent stage of senescence.

The relationship between upper epidermal and lower epidermal flavonols differed, similarly in both species, between green and yellow senescent leaves (Fig. S7). In green leaves, there was no correlation between the adaxial and abaxial flavonol content in *F. sylvatica* (R^2_{adj} =0.01 p = 0.101) or *B. pendula* (R^2_{adj} <0.01, p = 0.339), whereas in yellow leaves there was a strong positive correlation between flavonols measured on either side of the leaves in both species (*F. sylvatica* R^2_{adj}=0.40 p < 0.001 and *B. pendula* R^2_{adj} =0.54, p < 0.001*;* Fig. S7). This appears primarily to be due to a decrease in adaxial epidermal flavonols during leaf senescence which brought them down to similar levels as the abaxial flavonols (Fig. S7).

Mass Loss from Litter in the Controlled Experiment

During incubation, green leaves of both *B. pendula* and *F. sylvatica* lost more mass than yellow leaves (49% vs. 34%, F = 225, p = 0.003, Table 1). When response ratios to the dark treatments were compared for each species and leaf colour there was an overall effect of filter treatment on mass loss (Fig. 2, Table 2), but when compared separately the filter treatment only had a marginally non-significant effect on mass loss of green leaves of *F. sylvatica* (F= 2.6, p = 0.062, Table 1). In this case, leaves receiving the full spectrum in the chambers lost mass faster than those in the dark or under treatments where UV-A radiation and blue light were attenuated (Fig. 2, Table 1). Yellow leaves of *B. pendula* followed a similar pattern even though the effect was marginally non-significant (F = 2.3, p = 0.085, Fig. 2, Table 1).

Only yellow *B. pendula* leaves differed in mass loss according to leaf orientation (F= 11.05, p = 0.002, Fig. 2): leaves orientated with their abaxial epidermis facing the light source lost mass faster (0.05 - 0.10 % higher daily mass loss depending on the filter treatment) than leaves with their adaxial epidermis facing the light source (Fig. 2).

Mass Loss from Litter in the Forest Experiment

During decomposition in the forest stands green leaves of both *B. pendula* and *F. sylvatica* lost more mass than yellow leaves (65.0% against 34.2% and 35.2% against 16.2% respectively, F = 702, p = 0.001, Table 3), as was consistent with green and yellow leaves in the controlled experiment. The rate of mass loss was also slower in *F. sylvatica* than *B. pendula* (Fig. 3, species-by-colour interaction, F = 114, p = 0.009, Table 3). There were no differences in mass loss according to leaf orientation for either of the species and there was no interaction between the effects of filter treatments and leaf orientation (not shown). The filter treatment affected mass loss of (green-and-yellow) leaves of *F. sylvatica* and of green

leaves of *B. pendula,* and this effect differed according to the stand (significant Filter treatment-by-stand interactions; Fig 3, Table 3).

The effects of filter treatment were small and inconsistent among the stands. In green leaves of *F. sylvatica,* an effect of the filter treatment was found only in the *F. sylvatica* stand; where the No-UV treatment had a higher mass loss than the Full-spectrum treatment (pairwise comparison: No-UV – Full-spectrum $p = 0.031$, Table S5). For yellow leaf litter of *F. sylvatica,* there was no effect of filter treatment in the *A. platanoides* stand (Fig. 3, Table S5), while the other three stands presented contrasting results. In the *P. abies* and *F. sylvatica* stands, leaves exposed to Dark and No-UV/Blue treatments had higher daily mass loss then *F. sylvatica* litter exposed to the Full-spectrum and No-UV treatments (Fig. 3, Table S5), whereas in the *B. pendula* stand, the *F. sylvatica* litter exposed to the No-UV/Blue treatment had the highest mass loss (Fig. 3, Table S5).

For green leaf litter of *B. pendula* there was no effect of filter treatment in the *A. platanoides* stand (Fig. 3, Table S5). In the *F. sylvatica* stand, *B. pendula* litter exposed to the Dark treatment had higher daily mass loss then litter exposed to the Full-spectrum and No-UV treatments (Fig. 3, Table S5). In the *P. abies* stand, *B. pendula* litter exposed to Dark and Full-spectrum treatments had higher daily mass loss then litter exposed to the No-UV/Blue and No-UV treatments (Fig. 3, Table S5). In the *B. pendula* stand, the *B. pendula* litter exposed to the Full-Spectrum treatment had higher daily mass loss then litter exposed to the No-UV treatment (Fig. 3, Table S5).

Carbon and Nitrogen Content of Litter in the Controlled Experiment

Leaf C:N ratio as well as C and N concentration (henceforth [C] and [N]) significantly differed between species at the end of the photodegradation experiment (Table 2). There was a

364 significant interaction effect (Species x Leaf Colour) for [C], [N], and C:N ratio, meaning that
365 the response of yellow and green leaves varied with species (Table 2). At the end of our
366 photodegradation experiment, [C] was higher in yellow than green leaves of *B. pendula*, as
367 was the C:N ratio in leaves of both species. The difference between [N] of green and yellow
368 *B. pendula* leaves was much larger than that of *F. sylvatica* (Table 2). However, there was no
369 general response of leaf [N] to our filter treatments (Table 1), an effect was only apparent in
370 yellow leaves ($F = 4.71$, $p = 0.048$), where leaf orientation was also a significant factor ($F =$
371 3.41, $p = 0.027$, Fig. 4). Here, [N] was higher in yellow leaves of *B. pendula* with the adaxial
372 epidermis facing up (N = 1.25 % of dry weight, Fig. 4) than those leaves with the abaxial
373 epidermis facing up (N = 1.13 % of dry weight, Fig. 4). Considering pairwise interactions for
374 this effect, the [N] under the Full-Spectrum treatment was lower in those yellow leaves of *B.*
375 *pendula* with the abaxial epidermis facing up than those under the dark treatment (Table 2,
376 Fig. 4, $p = 0.012$).

377 ***Phenolic compounds from Leaf Litter after the Controlled Experiment***

378 We identified 29 phenolic compounds from green and yellow leaves of *Fagus sylvatica* and
379 16 from green and yellow leaves of *Betula pendula*. A comprehensive comparison of the
380 phenolic concentration and composition is given in Table S6 in the supplementary material,
381 while those compounds which responded to our treatments are illustrated in Fig. 5. At the
382 end of the experiment under controlled-irradiance treatments, the phenolic concentration
383 varied most with leaf colour and orientation (Table S7). Likewise, MDS mapping showed that
384 the composition of the phenolics profile of both species segregated primarily according to
385 leaf colour and then with leaf orientation, but not with filter treatment (Fig 6).

In *F. sylvatica* leaves, only three compounds were affected by our filter treatments: kaempferol 3-rhamnoside (F = 2.88, p = 0.046); neochlorogenic acid (F = 3.40, p = 0.025) and methanol (MeOH)-soluble condensed tannins in yellow leaves (F = 5.52, p = 0.002) (Table S7). The effect of filter treatment on the concentration of MeOH-soluble condensed tannins varied with the leaf colour (filter treatment x leaf colour interaction: F = 2.81, p = 0.049), being evident only in yellow leaves (Fig. 5). In this case, yellow leaves exposed to the Full-spectrum treatment had a lower content of MeOH-soluble condensed tannins than leaves expose to No-UVA/Blue treatment (pairwise comparison No-UVA/Blue - Full-Spectrum p = 0.009, Fig.5, Table S8). Kaempferol 3-rhamnoside was lower in leaves of *F. sylvatica* exposed to treatments excluding UV-A radiation and blue light than in leaves exposed to the full spectrum or under filters only excluding UV-A (pairwise comparisons: No-UVA/Blue - Full-Spectrum p = 0.037, No-UVA/Blue – No-UVA p = 0.042, Fig. 5, Table S8). Neochlorogenic acid was lower in leaves of *F. sylvatica* exposed to the Dark treatment than those exposed to the Full-spectrum treatment (pairwise comparisons: Dark – Full-spectrum p = 0.042, Fig. 5, Table S8).

In *B. pendula* leaves, only chlorogenic acid was affected by our filter treatments (F = 2.80, p = 0.050, Table S7), being lower in leaves exposed to the Dark and No-UVA/Blue treatments than treatments excluding only UV-A radiation (pairwise comparisons: Dark – No-UVA p = 0.029; No-UVA/Blue - No-UVA p = 0.035, Fig. 5, Table S9).

Discussion

In our study, species and stage of senescence were the main factors affecting litter decomposition. Compared to these factors, filter treatments had a minor effect both on mass loss and litter chemistry. The effects of our filter treatments on photodegradation in the controlled environments differed from their effects on decomposition in forest stands. While

409 the exclusion of solar UV radiation enhanced mass loss from leaf litter decomposing in the
410 forest stands, the presence of UV-A radiation in the controlled environment tended to
411 accelerate photodegradation. An increase in mass loss due to photodegradation in controlled
412 environments has also been reported for rice and wheat straws exposed to enhanced UV-A
413 [51] and UV-B radiation [52]. The effect of UV radiation did not transfer to decomposition
414 under equivalent filters in forest stands, a distinction that would be consistent with any effect
415 of sunlight photoinhibition on decomposers predominating over photochemical
416 mineralization during the initial 6 months of decomposition following leaf fall. An inhibitory
417 effect of sunlight on litter decomposition has also been reported for grass-litter
418 decomposition in sub-arctic environments [53]. However, in that environment when
419 equivalent litter was monitored in the same field site over a longer period of time (12-17
420 months), the effect of UV-B radiation on litter mass loss changed from negative to positive
421 [54]. Such a transition, attributed to a shift in the relative importance of different antagonistic
422 processes affected by UV radiation [52], may also occur in our forest stands over a longer
423 period of decomposition, but this remains untested. However, in a filter experiment in a
424 temperate forest, solar UV radiation accelerated decomposition of leaf litter from *Quercus*
425 *robur* and *F. sylvatica* over a 10-month period, but not of litter from *Fraxinus excelsior* over 7
426 months, under similar experimental treatments to ours but implemented later after leaf
427 senescence [55]. The treatment effects in our study may have differed over a longer period,
428 not only due to a changing role of photodegradation during different phases of decomposition
429 [53, 54], but also because of seasonal environmental changes including canopy closure which
430 reduces irradiance in the understorey and alters its spectral composition. In forest
431 environments, where decomposers principally determine the rate of decomposition, the
432 effect of direct photo-mineralization might be overridden by the capability of UV-B radiation

433 to inhibit microbial activity (photoinhibition) [20, 56]. In general, micro- and meso-fauna tend
434 to prefer darker environments [58, 59]; this is one likely reason for the high mass loss under
435 our dark treatment. This effect of filter treatments is consistent with that reported for *F.*
436 *excelsior* leaf litter under a similar combination of spectral-attenuation treatments in a moist-
437 temperate *F. sylvatica* forest [55]. The higher decomposition rates with increasing canopy
438 cover among our four stands, also supports this assertion (Table 3). On the other hand, the
439 lack of a UV-B radiation treatment in our controlled experiment could explain why we didn't
440 find an inhibitory effect of UV radiation on litter mass loss as reported elsewhere, e.g. with
441 *Pinus radiata* litter exposed to UV-B radiation [60]. While the radiation exposures in the two
442 experiments were largely well matched, there were greater fluctuations in temperature and
443 PAR in the forest environment due to sunflecks, especially during March and April. Sunlight is
444 relatively enriched in the green region (500-570 nm) in forest understoreys compared with
445 open environments (Fig.1C & 1D), which may have stimulated photomineralization or
446 photopriming while having few consequences on photoinhibition [12]. These differences in
447 exposure and the lack of interactive effects between different wavelengths might partially
448 explain the different results obtained in the two experiments. Moreover, temperature
449 conditions in the forest stands and in the controlled experiment differed, with the forest
450 environment presenting a higher temperature fluctuation daily, and over the 6 months of the
451 experiment (Fig. S9), while in the controlled environment the temperature was kept constant
452 during the experiment with only small day-night variations (Fig, S5).

453 ***Leaf biochemistry and photodegradation***

454 The results of both experiments confirmed our expectations that green leaves would
455 decompose faster than yellow leaves in both species. The higher content of N-rich Rubisco,
456 chlorophyll and other photosynthetic pigments in green leaf litter makes it more palatable

457 [61] for decomposers than fully senesced leaves, allowing faster decomposition[27].
458 Senescent and green leaves differ in their nutrients content due to the process of nutrient
459 reabsorption, which takes place during leaf senescence [62, 63]. This results in fewer low
460 molecular phenolics and accumulation of tannins in senescent leaves [64, 65]. A result
461 consistent with the higher concentration of condensed tannins and fewer low-molecular
462 phenolics in senescent leaves than leaves that were harvested when still green in our study.
463 Tannins reduce the rate of litter decomposition in various woody species, by binding proteins
464 and simple polymers making them unavailable for microbial decomposition [66-68]. It is
465 worth noting, however, that flavonoids isolated through HPLC after photodegradation, were
466 higher in *F. sylvatica* leaves harvested when yellow than those harvested when green. This
467 might suggest an increase in flavonoid concentration during leaf senescence, as recently
468 reported for several tree species by [25]. However, it contradicts the decrease in upper
469 epidermal flavonols measured with the Dualex before the experiment in yellow leaves
470 compared with green leaves of *F. sylvatica* (Fig. S7). This change, specific to the adaxial
471 epidermis, might suggest that flavonols are translocated from the vacuoles of epidermal cells
472 elsewhere in the leaf rather than broken down during senescence.

473 The exposure of leaves to UV radiation during the growing season causes the accumulation
474 of photoprotective pigments, mainly flavonoids, in leaf adaxial epidermis which reduces the
475 penetration of sunlight and particularly UV radiation into leaf tissues [69-71], potentially
476 protecting the mesophyll from photodegradation effects [14]. The accumulation of these
477 photoprotective pigments, as a consequence of UV exposure, has been reported to alter litter
478 chemistry of *Alnus* sp. and *Betula* sp. and consequently impact decomposition through an
479 effect on microbial communities and soil respiration [24]. By taking Dualex measurements of
480 the same leaves before and after drying, we confirmed that differences in optical properties

481 attributed to epidermal flavonols were conserved in dried leaves (Fig. S1), meaning that the
482 differences between upper and lower epidermal screening are likely to alter the penetration
483 of UV within the leaf during photodegradation. However, we only found an effect of leaf
484 orientation on mass loss and [N] in yellow leaves of *B. pendula* in the controlled environment
485 experiment. This effect would be consistent with reduced microbial colonisation on these
486 leaves, which we also considered a viable explanation for the filter effect found in the forest
487 stands. However, lack of association between effects on [N] and mass loss in the controlled
488 experiment would imply that direct photodegradation is the dominant process. Nevertheless,
489 the phenolic profile of leaves recorded after the photodegradation experiment segregated
490 clearly with leaf orientation, and orientation had an effect on the content of some of the
491 flavonoids isolated with the HPLC analysis in *F. sylvatica* leaves (Figs. 5 and 6). Taken together,
492 these results suggest that the spatial distribution of flavonoids within the leaves, affecting
493 their optical properties and the penetration of UV radiation, can have an effect on
494 photodegradation. However, these effects were too small, or the duration of exposure to our
495 irradiance treatments was insufficient, to produce an effect of orientation that could be
496 quantified in terms of mass loss, [N] or [C]. Such a test might be more informative with clonal
497 leaf material from plants grown under fully standardised conditions, where comparable initial
498 phenolic profiles would provide a consistent baseline prior to decomposition.

499 ***The role of photodegradation in initial decomposition in the forest understorey***
500 After 6 months of decomposition in the forest, the mass loss was about 35.2% and 16.2% for
501 green and yellow leaves of *Fagus sylvatica*, and 65.0% and 34.2% for green and yellow leaves
502 of *Betula pendula* respectively. This scale of mass loss from senescent leaves was reasonable,
503 compared with that reported in other studies in similar environments after 6 months of
504 decomposition: 15-20% for *F. sylvatica* litter and 40-45% for *B. pendula* litter [72, 73]. In our

505 forest decomposition experiment, where adjacent stands were selected to form a gradient of
506 LAI, litter mass loss was affected by stand type. This might suggest that even in southern
507 Finland, where winter irradiances are low, the light environment created by different
508 canopies can affect litter decomposition. Mass loss was highest from the *Picea abies* stand in
509 our experiment (Table S10). But since the understorey in this stand received both the lowest
510 irradiance and the highest amount of blue light (Table S3) over the 6 months of the
511 experiment, either spectral composition or total irradiance or both, could be responsible for
512 this result. This would be in agreement with previous studies that proved the importance of
513 blue light in the process of photodegradation [12, 43]. Stands with high canopy density also
514 intercept more precipitation in the form of snow, leading to smaller snow depths and
515 consequently modifying soil temperature and moisture [74-76]. Since forest canopies also
516 affect a variety of micro-environmental conditions such as temperature, water availability,
517 soil characteristics and decomposer assemblages, any effect of light environment on
518 decomposition will operate in combination with these factors [77-79]. We found no evidence
519 for home-field advantage; the theory that litter from a particular forest decomposes fastest
520 in its own stand irrespective of conditions because of its specialised decomposer assemblage
521 [80, 81], e.g. *Betula pendula* litter in the *Betula pendula* stand. However, further investigation
522 is needed, both in controlled and forest environments, to assess the relative importance of
523 photodegradation compared with other environmental factors in litter decomposition at high
524 latitudes and over longer experimental periods.

525 **Conclusions**

526 This study revealed that photodegradation can play a role in surface leaf litter decomposition
527 in forest ecosystems at high latitudes, but this role was not consistent with photodegradation
528 produced by UV-A radiation and blue light under controlled conditions. There, UV-A radiation

and blue light accelerated mass loss, while in forest stands decomposition was generally slightly slower under filters transmitting UV radiation and blue light. The contribution of photodegradation to decomposition was relatively small, and varied according to the canopy tree species, the leaf litter species and leaf traits related to stage of leaf senescence.

Acknowledgements

We are grateful to Anu Heikkilä (for the UV data) and FMI for diffuse direct irradiance/cloudiness data, and Viikki Arboretum and Experiment Plots of the University of Helsinki managed by Daniel Richterich, for allowing use of the experimental sites, and provision of meteorological station data from their *in situ* weather station and Pedro José Aphalo's weather station. This research was funded by Academy of Finland decisions #266523 and #304519 to TMR, and a grant from the Region "Haute-Normandie" through the GRR-TERA SCALE (UFOSE Project) to MP.

References

[1] M.J. Swift, O.W. Heal, J.M. Anderson, J. Anderson, Decomposition in terrestrial ecosystems, Univ of California Press, 1979.

[2] P. Sulkava, V. Huhta, Effects of hard frost and freeze-thaw cycles on decomposer communities and N mineralisation in boreal forest soil, Applied Soil Ecology, 22 (2003) 225-239.

[3] F.S. Chapin III, P.A. Matson, H.A. Mooney, Principles of terrestrial ecosystem ecology., Springer-Verlag. , New York, 2002.

[4] J. Liski, A. Nissinen, M. Erhard, O. Taskinen, Climatic effects on litter decomposition from arctic tundra to tropical rainforest, Global Change Biology, 9 (2003) 575-584.

[5] J. Zhu, W. Yang, X.J.P.o. He, Temporal dynamics of abiotic and biotic factors on leaf litter of three plant species in relation to decomposition rate along a subalpine elevation gradient, PLoS ONE, 8 (2013) e62073.

[6] E. Paudel, G.G.O. Dossa, M. de Blécourt, P. Beckschäfer, J. Xu, R.D. Harrison, Quantifying the factors affecting leaf litter decomposition across a tropical forest disturbance gradient, Ecosphere, 6 (2015) 1-20.

[7] W. Parton, W.L. Silver, I.C. Burke, L. Grassens, M.E. Harmon, W.S. Currie, J.Y. King, E.C. Adair, L.A. Brandt, S.C. Hart, B. Fasth, Global-Scale Similarities in Nitrogen Release Patterns During Long-Term Decomposition, Science, 315 (2007) 361.

[8] D.A. Perry, R. Oren, S.C. Hart, Forest ecosystems 2nd ed., The Johns Hopkins University Press, Baltimore, 2008.

[9] F.-X. Joly, A. Milcu, M. Scherer-Lorenzen, L.-K. Jean, F. Bussotti, S.M. Dawud, S. Müller, M. Pollastrini, K. Raulund-Rasmussen, L. Vesterdal, S. Hättenschwiler, Tree species diversity affects decomposition through modified micro-environmental conditions across European forests, New Phytologist, 214 (2017) 1281-1293.

[10] K.I. Predick, S.R. Archer, S.M. Aguillon, D.A. Keller, H.L. Throop, P.W. Barnes, UV-B radiation and shrub canopy effects on surface litter decomposition in a shrub-invaded dry grassland, Journal of Arid Environments, 157 (2018) 13-21.

[11] A.T. Austin, L. Vivanco, Plant litter decomposition in a semi-arid ecosystem controlled by photodegradation, Nature, 442 (2006) 555.

[12] A.T. Austin, M.S. Méndez, C.L. Ballaré, Photodegradation alleviates the lignin bottleneck for carbon turnover in terrestrial ecosystems, Proceedings of the National Academy of Sciences, 113 (2016) 4392.

[13] J.Y. King, L.A. Brandt, E.C.J.B. Adair, Shedding light on plant litter decomposition: advances, implications and new directions in understanding the role of photodegradation, Biogeochemistry, 111 (2012) 57-81.

[14] P.W. Barnes, H.L. Throop, S.R. Archer, D.D. Breshears, R.L. McCulley, M.A. Tobler, Sunlight and Soil–Litter Mixing: Drivers of Litter Decomposition in Drylands, in: U. Lüttge, W. Beyschlag (Eds.) Progress in Botany: Vol. 76, Springer International Publishing, Cham, 2015, pp. 273-302.

[15] S. Madronich, R.L. McKenzie, L.O. Björn, M.M. Caldwell, Changes in biologically active ultraviolet radiation reaching the Earth's surface, Journal of Photochemistry and Photobiology B: Biology, 46 (1998) 5-19.

[16] J.F. Bornman, P.W. Barnes, S.A. Robinson, C.L. Ballare, S. Flint, M.M.J.P. Caldwell, P. Sciences, Solar ultraviolet radiation and ozone depletion-driven climate change: effects on terrestrial ecosystems, Photochemical & Photobiological Sciences, 14 (2015) 88-107.

[17] B.K. Sercu, L. Baeten, F. van Coillie, A. Martel, L. Lens, K. Verheyen, D. Bonte, How tree species identity and diversity affect light transmittance to the understory in mature temperate forests, Ecology and Evolution, 7 (2017) 10861-10870.

[18] E. Erdenebileg, X. Ye, C. Wang, Z. Huang, G. Liu, J.H.C. Cornelissen, Positive and negative effects of UV irradiance explain interaction of litter position and UV exposure on litter decomposition and nutrient dynamics in a semi-arid dune ecosystem, Soil Biology and Biochemistry, 124 (2018) 245-254.

[19] S.M. Hartikainen, A. Jach, A. Grané, T.M. Robson, Assessing scale-wise similarity of curves with a thick pen: As illustrated through comparisons of spectral irradiance, Ecology and Evolution, 8 (2018) 10206-10218.
[20] J.F. Bornman, P.W. Barnes, T.M. Robson, S.A. Robinson, M.A. Jansen, C.L. Ballaré, S.D. Flint, Linkages between stratospheric ozone, UV radiation and climate change and their implications for terrestrial ecosystems, Photochemical & Photobiological Sciences, 18 (2019) 681-716.
[21] B. Hoorens, R. Aerts, M.J.O. Stroetenga, Does initial litter chemistry explain litter mixture effects on decomposition?, Ecosystem Ecology, 137 (2003) 578-586.
[22] T.A. Day, M.S. Bliss, A.R. Tomes, C.T. Ruhland, R. Guénon, Desert leaf litter decay: Coupling of microbial respiration, water-soluble fractions and photodegradation, Global Change Biology, 24 (2018) 5454-5470.
[23] G. Liu, L. Wang, L. Jiang, X. Pan, Z. Huang, M. Dong, J.H.C. Cornelissen, Specific leaf area predicts dryland litter decomposition via two mechanisms, Journal of Ecology, 106 (2018) 218-229.
[24] T. Kotilainen, J. Haimi, R. Tegelberg, R. Julkunen-Tiitto, E. Vapaavuori, P.J. Aphalo, Solar ultraviolet radiation alters alder and birch litter chemistry that in turn affects decomposers and soil respiration, Oecologia, 161 (2009) 719-728.
[25] H. Mattila, D. Valev, M. Antinluoma, O. Virtanen, S. Khorobrykh, V. Havurinne, E. Tyystjärvi, K.B. Mishra, Degradation of chlorophyll and synthesis of flavonols during autumn senescence—the story told by individual leaves, AoB PLANTS, 10 (2018).
[26] W.A. Hoch, E.L. Zeldin, B.H. McCown, Physiological significance of anthocyanins during autumnal leaf senescence, Tree Physiology, 21 (2001) 1-8.
[27] J.H.C. Cornelissen, An Experimental Comparison of Leaf Decomposition Rates in a Wide Range of Temperate Plant Species and Types, Journal of Ecology, 84 (1996) 573-582.
[28] T.A. DAY, G. MARTIN, T.C. VOGELMANN, Penetration of UV-B radiation in foliage: evidence that the epidermis behaves as a non-uniform filter, Plant, Cell & Environment, 16 (1993) 735-741.
[29] T. Ahti, L. Hämet-Ahti, J. Jalas, Vegetation zones and their sections in northwestern Europe, in: Annales Botanici Fennici, JSTOR, 1968, pp. 169-211.
[30] C.A. Schneider, W.S. Rasband, K.W.J.N.m. Eliceiri, NIH Image to ImageJ: 25 years of image analysis, Nature Methods, 9 (2012) 671.
[31] F. Wang, SIOX plugin in ImageJ: area measurement made easy., UV4Plants Bulletin, 2 (2017) 37-44.
[32] E.E. Pfündel, N. Ben Ghozlen, S. Meyer, Z.G.J.P.R. Cerovic, Investigating UV screening in leaves by two different types of portable UV fluorimeters reveals in vivo screening by anthocyanins and carotenoids, Photosynthesis Research, 93 (2007) 205-221.
[33] Z.G. Cerovic, G. Masdoumier, N.B. Ghozlen, G. Latouche, A new optical leaf-clip meter for simultaneous non-destructive assessment of leaf chlorophyll and epidermal flavonoids, Physiologia Plantarum, 146 (2012) 251-260.
[34] C.C. Brelsford, L.O. Morales, J. Nezval, T.K. Kotilainen, S.M. Hartikainen, P.J. Aphalo, T.M. Robson, Do UV-A radiation and blue light during growth prime leaves to cope with acute high light in photoreceptor mutants of Arabidopsis thaliana?, Physiologia Plantarum, 0 (2018).
[35] C.C. Brelsford, L.O. Morales, J. Nezval, T.K. Kotilainen, S.M. Hartikainen, P.J. Aphalo, T.M. Robson, Do UV-A radiation and blue light during growth prime leaves to cope with acute high light in photoreceptor mutants of Arabidopsis thaliana?, Physiologia Plantarum, 165 (2019) 537-554.
[36] P.J. Aphalo, Quantification of UV Radiation, in: B.R. Jordan (Ed.) UV-B Radiation and Plant Life: Molecular Biology to Ecology, CAB International, Oxford, UK, 2017, pp. 10-22.
[37] P.J. Aphalo, T.M. Robson, J. Piiparinen, How to check an array spectrometer., Int. Assoc. Plant UV Res., updated June 2, 2013, accessed November 11, 2017. (2016).
[38] P.J. Aphalo, A. Albert, A. McLeod, A. Heikkilä, I. Gómez, F. López Figueroa, T.M. Robson, Å. Strid, Beyond the visible: a handbook of best practice in plant UV photobiology, 1st ed., University of Helsinki, Division of Plant Biology, Helsinki, 2012.

[39] P. Schleppi, M. Conedera, I. Sedivy, A. Thimonier, Correcting non-linearity and slope effects in the estimation of the leaf area index of forests from hemispherical photographs, Agricultural and Forest Meteorology, 144 (2007) 236-242.
[40] A. Thimonier, I. Sedivy, P. Schleppi, Estimating leaf area index in different types of mature forest stands in Switzerland: a comparison of methods, European Journal of Forest Research, 129 (2010) 543-562.
[41] J.S. Mäkelä, K. Lakkala, T. Koskela, T. Karppinen, J.M. Karhu, V. Savastiouk, H. Suokanerva, J. Kaurola, A. Arola, A.V. Lindfors, O. Meinander, G. de Leeuw, A. Heikkilä, Data flow of spectral UV measurements at Sodankylä and Jokioinen, Geosci. Instrum. Method. Data Syst., 5 (2016) 193-203.
[42] A. Heikkilä, J.S. Mäkelä, K. Lakkala, O. Meinander, J. Kaurola, T. Koskela, J.M. Karhu, T. Karppinen, E. Kyrö, G.d. Leeuw, In search of traceability: two decades of calibrated Brewer UV measurements in Sodankylä and Jokioinen, Geosci. Instrum. Method. Data Syst., 5 (2016) 531-540.
[43] M. Pieristè, M. Chauvat, T.K. Kotilainen, A.G. Jones, M. Aubert, T.M. Robson, E. Forey, Solar UV-A radiation and blue light enhance tree leaf litter decomposition in a temperate forest, Oecologia, (2019) 1-13.
[44] A.L. Kolstad, J. Asplund, M.-C. Nilsson, M. Ohlson, L. Nybakken, Soil fertility and charcoal as determinants of growth and allocation of secondary plant metabolites in seedlings of European beech and Norway spruce, Environmental and Experimental Botany, 131 (2016) 39-46.
[45] A. Hagerman, Tanin Chemistry Handbook, Maiami: Oxford university, 2002.
[46] J. Oksanen, F.G. Blanchet, R. Kindt, P. Legendre, P.R. Minchin, R. O'hara, G.L. Simpson, P. Solymos, M.H.H. Stevens, H. Wagner, vegan: Community Ecology Package - version 2.5-4, in, 2019.
[47] H. Wickham, ggplot2: Elegant Graphics for Data Analysis Springer-Verlag New York, in, Version, 2009.
[48] P.J. Aphalo, Learn R... as you learnt your mother tongue, Leanpub, Helsinki, Finland, 2016.
[49] P.J. Aphalo, The R4photobiology Suite: Spectral Irradiance, UV4Plants Bulletin, 2015 No 1 (2015) 21-29.
[50] R-Core-Team, R: A language and environment for statistical computing. , in, R Foundation for Statistical Computing, Vienna, Austria, 2018.
[51] Y. Li, H. Huang, G. Wu, S. Yan, Z. Chang, J. Bi, L. Chen, The Effects of UV-A on Dry Rice Straw Decomposition under Controlled Laboratory Conditions, BioResources, 11 (2016).
[52] G. Zhou, J. Zhang, J. Mao, C. Zhang, L. Chen, X. Xin, B. Zhao, Mass loss and chemical structures of wheat and maize straws in response to ultraviolet-B radiation and soil contact, Scientific Reports, 5 (2015) 14851.
[53] V.A. Pancotto, O.E. Sala, M. Cabello, N.I. López, T. Matthew Robson, C.L. Ballaré, M.M. Caldwell, A.L. Scopel, Solar UV-B decreases decomposition in herbaceous plant litter in Tierra del Fuego, Argentina: potential role of an altered decomposer community, Global Change Biology, 9 (2003) 1465-1474.
[54] V.A. Pancotto, O.E. Sala, T.M. Robson, M.M. Caldwell, A.L. Scopel, Direct and indirect effects of solar ultraviolet-B radiation on long-term decomposition, Global Change Biology, 11 (2005) 1982-1989.
[55] M. Pieristè, M. Chauvat, T.K. Kotilainen, A.G. Jones, M. Aubert, T.M. Robson, E. Forey, Solar UV-A radiation and blue light enhance tree leaf litter decomposition in a temperate forest, *minor revision in* Oecologia, (2019).
[56] A.F. Bais, R.M. Lucas, J.F. Bornman, C.E. Williamson, B. Sulzberger, A.T. Austin, S.R. Wilson, A.L. Andrady, G. Bernhard, R.L. McKenzie, Environmental effects of ozone depletion, UV radiation and interactions with climate change: UNEP Environmental Effects Assessment Panel, update 2017, Photochemical and Photobiological Sciences, 17 (2018) 127-179.
[58] Y. Lin, S.D. Karlen, J. Ralph, J.Y. King, Short-term facilitation of microbial litter decomposition by ultraviolet radiation, Science of The Total Environment, 615 (2018) 838-848.
[59] J. Wang, L. Liu, X. Wang, Y. Chen, The interaction between abiotic photodegradation and microbial decomposition under ultraviolet radiation, Global Change Biology, 21 (2015) 2095-2104.

692 [60] M.U.F. Kirschbaum, S.M. Lambie, H. Zhou, No UV enhancement of litter decomposition
693 observed on dry samples under controlled laboratory conditions, Soil Biology and Biochemistry, 43
694 (2011) 1300-1307.
695 [61] M. Schädler, G. Jung, H. Auge, R. Brandl, Palatability, decomposition and insect herbivory:
696 patterns in a successional old-field plant community, Oikos, 103 (2003) 121-132.
697 [62] J. Simon, V.M. Dörken, A. L.-M.-Arnold, B. Adamczyk, Environmental Conditions and Species
698 Identity Drive Metabolite Levels in Green Leaves and Leaf Litter of 14 Temperate Woody Species,
699 Forests, 9 (2018) 775.
700 [63] I.J. Wright, M. Westoby, Nutrient concentration, resorption and lifespan: leaf traits of Australian
701 sclerophyll species, Functional Ecology, 17 (2003) 10-19.
702 [64] S. Hättenschwiler, P.M. Vitousek, The role of polyphenols in terrestrial ecosystem nutrient
703 cycling, Trends in Ecology & Evolution, 15 (2000) 238-243.
704 [65] J. Koricheva, K.E. Barton, Temporal changes in plant secondary metabolite production: patterns,
705 causes and consequences., in: D.M. Iason GR, Hartley SE (Ed.) The ecology of plant secondary
706 metabolites., Cambridge University Press, Cambridge, 2012, pp. 10-33.
707 [66] S. Hättenschwiler, H.B. Jørgensen, Carbon quality rather than stoichiometry controls litter
708 decomposition in a tropical rain forest, Journal of Ecology, 98 (2010) 754-763.
709 [67] J.P. Schimel, K.V. Cleve, R.G. Cates, T.P. Clausen, P.B. Reichardt, Effects of balsam poplar
710 (Populus balsamifera) tannins and low molecular weight phenolics on microbial activity in taiga
711 floodplain soil: implications for changes in N cycling during succession, Canadian Journal of Botany,
712 74 (1996) 84-90.
713 [68] J.A. Schweitzer, J.K. Bailey, B.J. Rehill, G.D. Martinsen, S.C. Hart, R.L. Lindroth, P. Keim, T.G.
714 Whitham, Genetically based trait in a dominant tree affects ecosystem processes, Ecology Letters, 7
715 (2004) 127-134.
716 [69] L.G. Landry, C.C.S. Chapple, R.L. Last, Arabidopsis Mutants Lacking Phenolic Sunscreens Exhibit
717 Enhanced Ultraviolet-B Injury and Oxidative Damage, Plant Physiology, 109 (1995) 1159.
718 [70] T.A. Day, T.C. Vogelmann, Alterations in photosynthesis and pigment distributions in pea leaves
719 following UV-B exposure, Photobiophysics and photosynthesis, 94 (1995) 433-440.
720 [71] M.A.K. Jansen, V. Gaba, B.M. Greenberg, Higher plants and UV-B radiation: balancing damage,
721 repair and acclimation, Trends in Plant Science, 3 (1998) 131-135.
722 [72] M. Portillo-Estrada, M. Pihlatie, J.F. Korhonen, J. Levula, A.K. Frumau, A. Ibrom, J.J. Lembrechts,
723 L. Morillas, L. Horváth, S.K. Jones, Climatic controls on leaf litter decomposition across European
724 forests and grasslands revealed by reciprocal litter transplantation experiments, Biogeosciences, 13
725 (2016) 1621-1633.
726 [73] T. Silfver, J. Mikola, M. Rousi, H. Roininen, E. Oksanen, Leaf Litter Decomposition Differs among
727 Genotypes in a Local Betula pendula Population, Oecologia, 152 (2007) 707-714.
728 [74] P.-E. Mellander, H. Laudon, K. Bishop, Modelling variability of snow depths and soil
729 temperatures in Scots pine stands, Agricultural and Forest Meteorology, 133 (2005) 109-118.
730 [75] J. Pomeroy, B. Goodison, Winter and Snow, in: T. Oke, W.R. Rouse, W.G. Bailey (Eds.) The
731 surface climates of Canada, McGill-Queen's University Press, 1997, pp. 68-100.
732 [76] R. Davis, J. Hardy, W. Ni, C. Woodcock, J. McKenzie, R. Jordan, X. Li, Variation of snow cover
733 ablation in the boreal forest: A sensitivity study on the effects of conifer canopy, Journal of
734 Geophysical Research: Atmospheres, 102 (1997) 29389-29395.
735 [77] L. Augusto, A. De Schrijver, L. Vesterdal, A. Smolander, C. Prescott, J. Ranger, Influences of
736 evergreen gymnosperm and deciduous angiosperm tree species on the functioning of temperate and
737 boreal forests, Biological Reviews, 90 (2014) 444-466.
738 [78] B. Kovács, F. Tinya, P. Ódor, Stand structural drivers of microclimate in mature temperate mixed
739 forests, Agricultural and Forest Meteorology, 234 (2017) 11-21.
740 [79] F. Zellweger, D. Coomes, J. Lenoir, L. Depauw, S.L. Maes, M. Wulf, K.J. Kirby, J. Brunet, M.
741 Kopecký, F. Máliš, Seasonal drivers of understorey temperature buffering in temperate deciduous

742 forests across Europe, Global Ecology and Biogeography, (2019) 00: 1– 13.
743 https://doi.org/10.1111/geb.12991.
744 [80] E. Ayres, H. Steltzer, B.L. Simmons, R.T. Simpson, J.M. Steinweg, M.D. Wallenstein, N. Mellor,
745 W.J. Parton, J.C. Moore, D.H.J.S.B. Wall, Home-field advantage accelerates leaf litter decomposition
746 in forests, Soil Biology and Biochemistry, 41 (2009) 606-610.
747 [81] J. Asplund, H. Kauserud, S. Bokhorst, M.H. Lie, M. Ohlson, L. Nybakken, Fungal communities
748 influence decomposition rates of plant litter from two dominant tree species, Fungal Ecology, 32
749 (2017) 1-8.

750

Figures

Figure 1: Spectral treatments created by selective attenuation of radiation by plastic filters in experiments under (A) controlled and (B) sunlight conditions. Measurements (B) in full sun between 9:00-9:25 a.m. on October 4th 2016 in Viikki field site. Measurements of (C) sunfleck and (D) shade spectra from each of the forest stands.

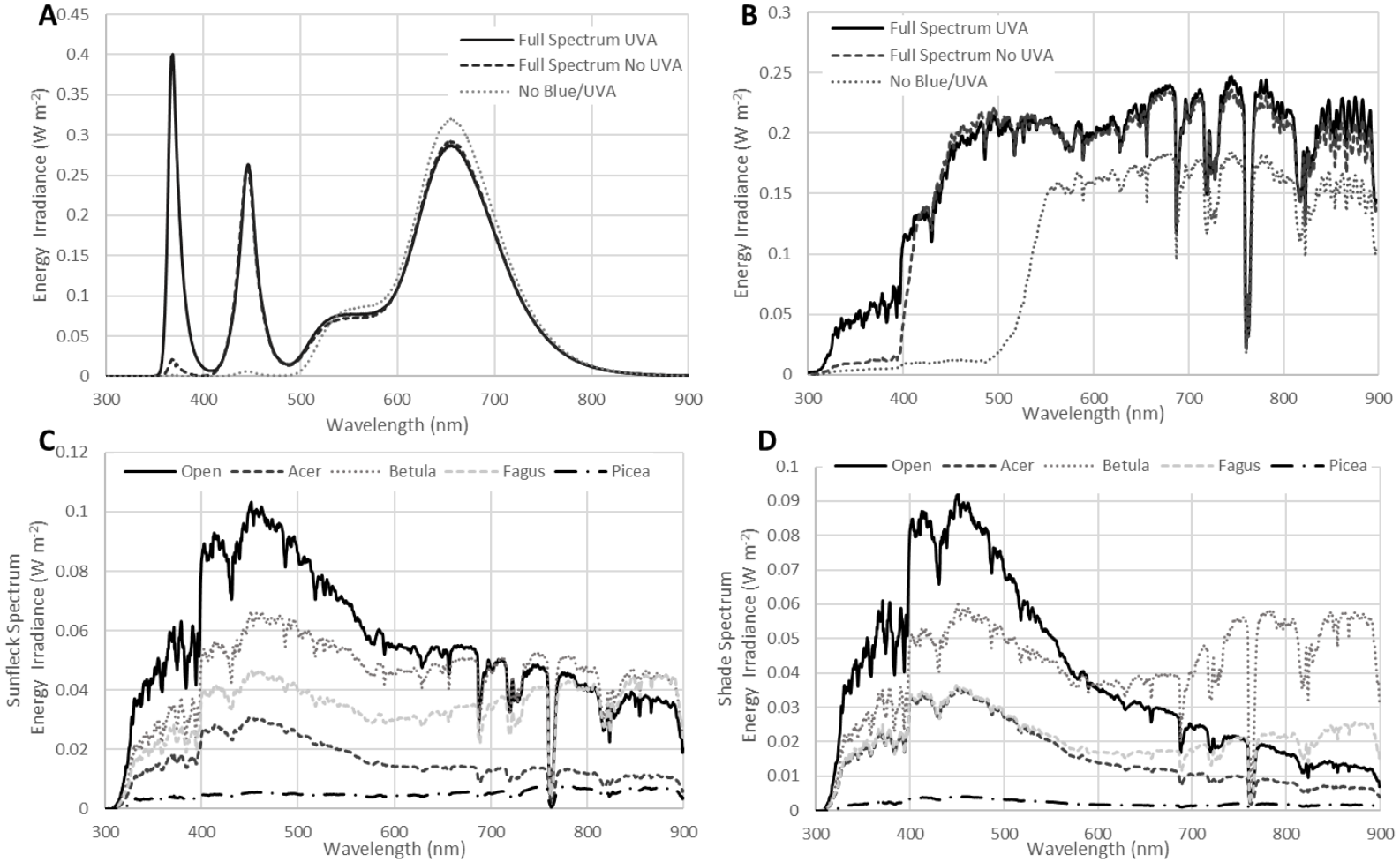

Figure 2: The response ratio of average daily % mass loss from leaves under each filter treatment over the duration of the controlled environment. Panels separate for green and yellow leaves of *B. pendula* and *F. sylvatica.* Table 2 gives ANOVA results and means values. Leaf orientation, (adaxial [▲] or abaxial [■] epidermis facing upwards toward the lamps) had no significant effect apart from in Yellow Leaves of *Betula pendula* (F = 11.05, *p* = 0.002), for which significant pair-wise interactions between filters for "lower up" leaves are distinguished with lower case letters. Upper case letters denote significant pairwise interactions among filter treatments for green leaves of *F. sylvatica*.

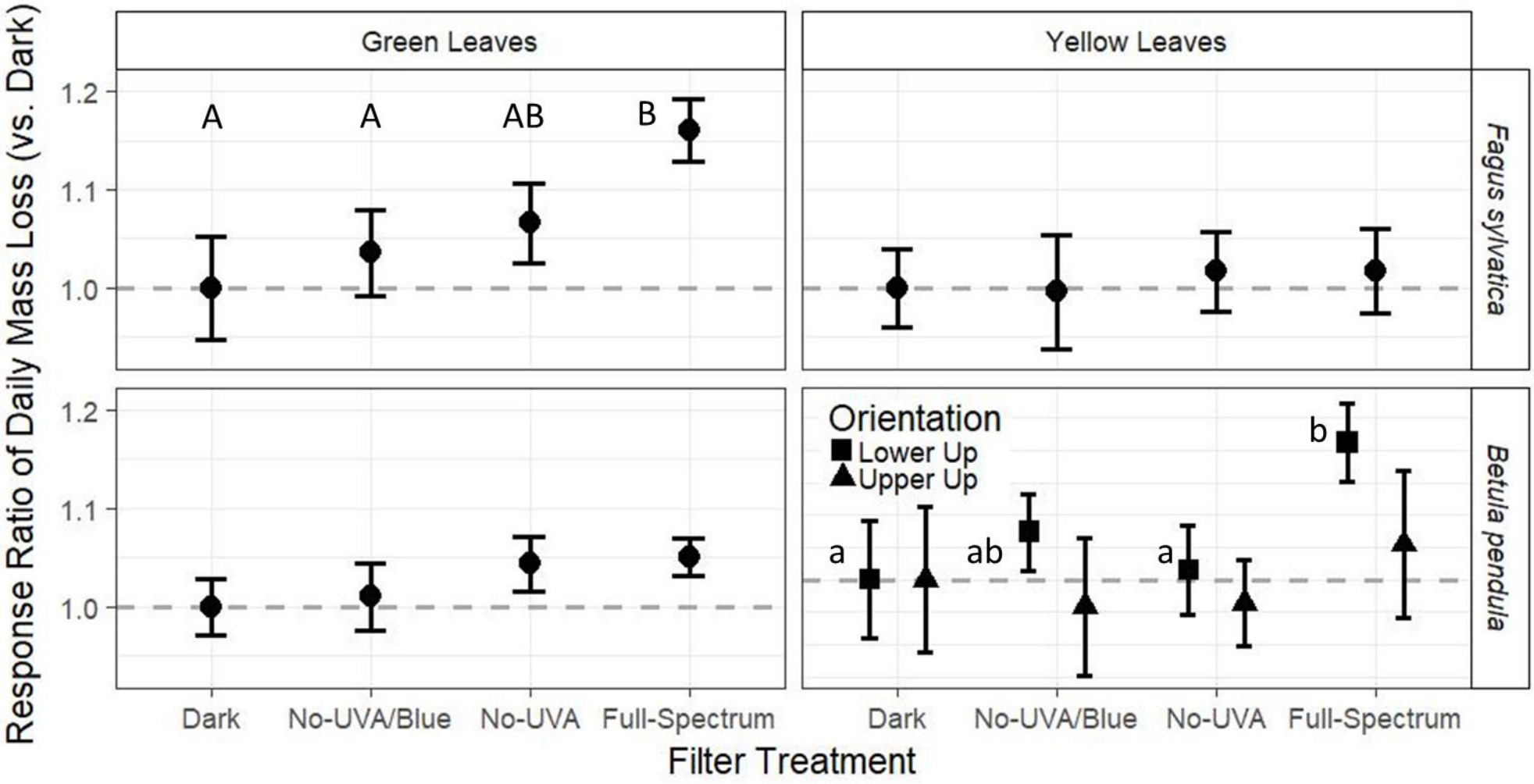

Figure 3: The response ratio of average daily mass loss of leaf litter under each filter treatment, decomposing in different forest stands. Table 3 gives ANOVA results and means values. Lower case letters denote significant differences between filter treatments within the same stand for those three species-by-leaf-colour combinations where there was a significant effect of filter treatment.

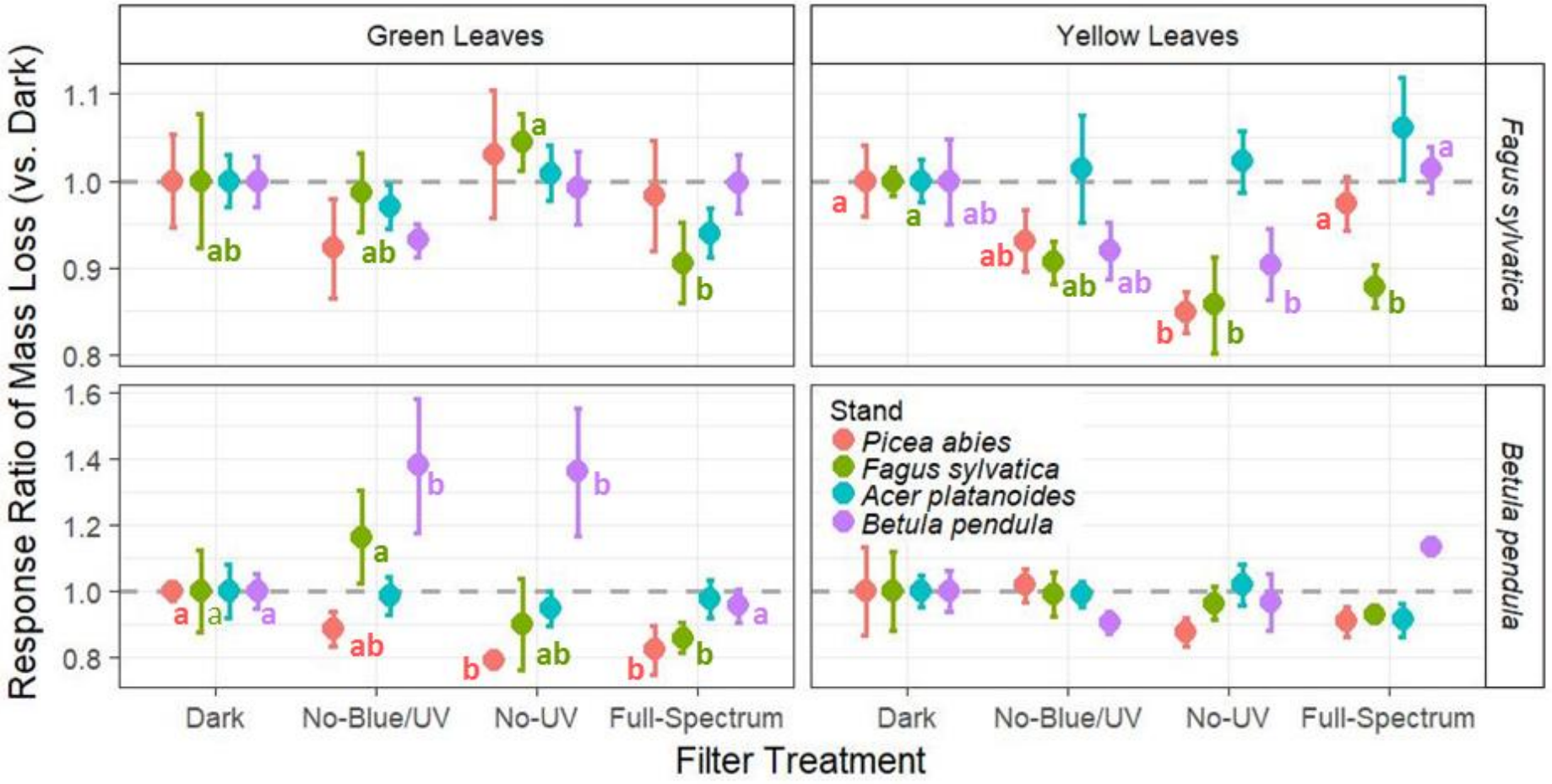

Figure 4: The response ratio of N content of leaf litter under each filter treatment at the end of the controlled conditions photodegradation experiment. Table 2 gives ANOVA results and means values. Leaf orientation, (adaxial [▲] or abaxial [■] epidermis facing upwards toward the lamps) had no significant effect apart from in Yellow Leaves of *Betula pendula* (F = 4.71, *p* = 0.048), for which significant differences between pairs of filters for "lower up" leaves are distinguished with lower case letters. The equivalent response ratios of C content and C:N ratio are given in Fig. S8.

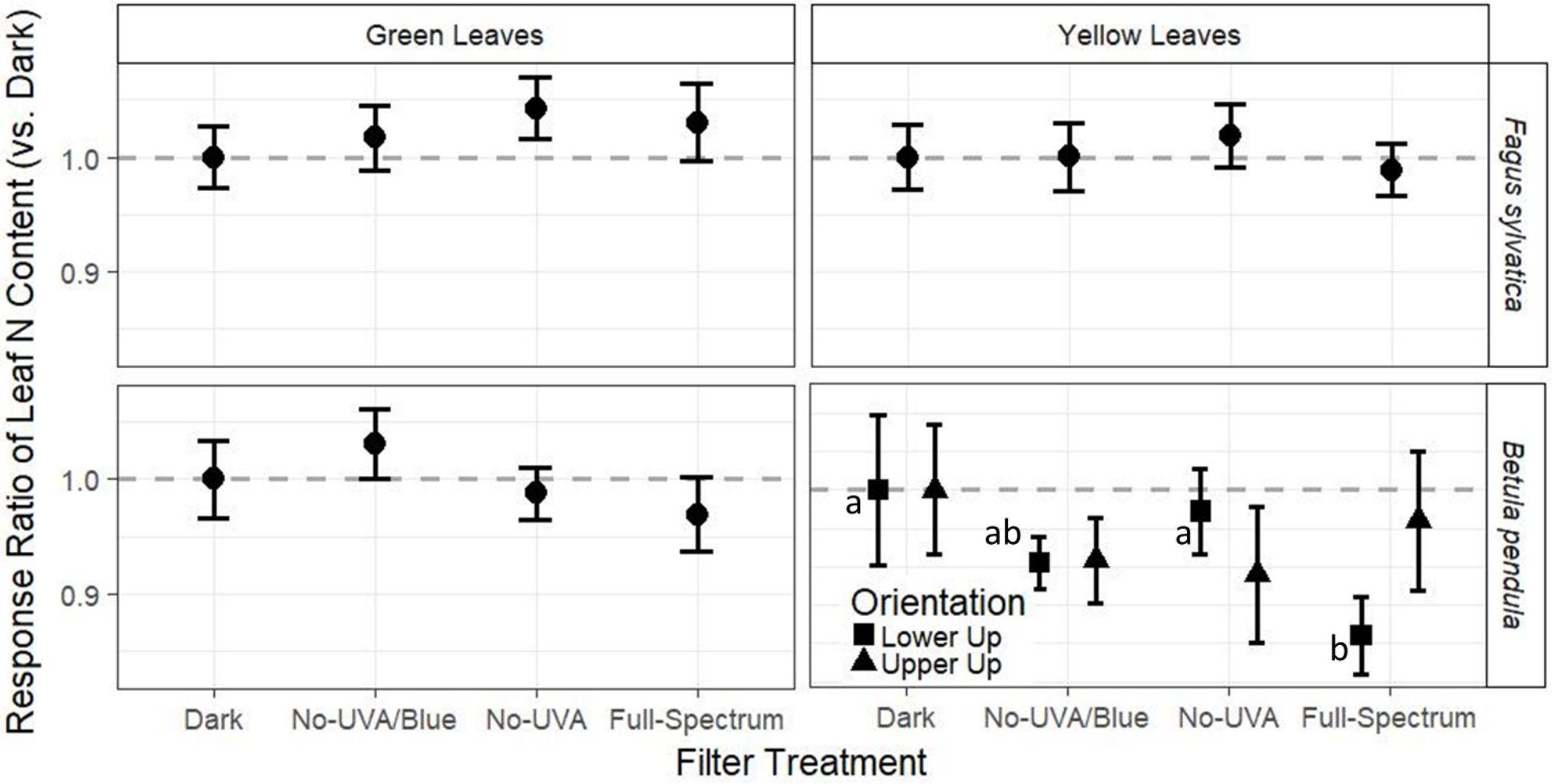

Figure 5: Phenolic compounds in senescent yellow and green leaves of Fagus sylvatica and Betula pendula following 10 weeks of photdegradation under our filter treatments. Mean and SE are shown. Upper case letters show significant difference between pairs of filter treatments, "ns" stands for "non-significant, lower case letters indicate significant differences between pairs of filter treatments in yellow leaves (filter treatment x leaf colour interaction). Only compounds which responded to our treatment are displayed here, the complete leaf phenolic profiles are given in Table S7.

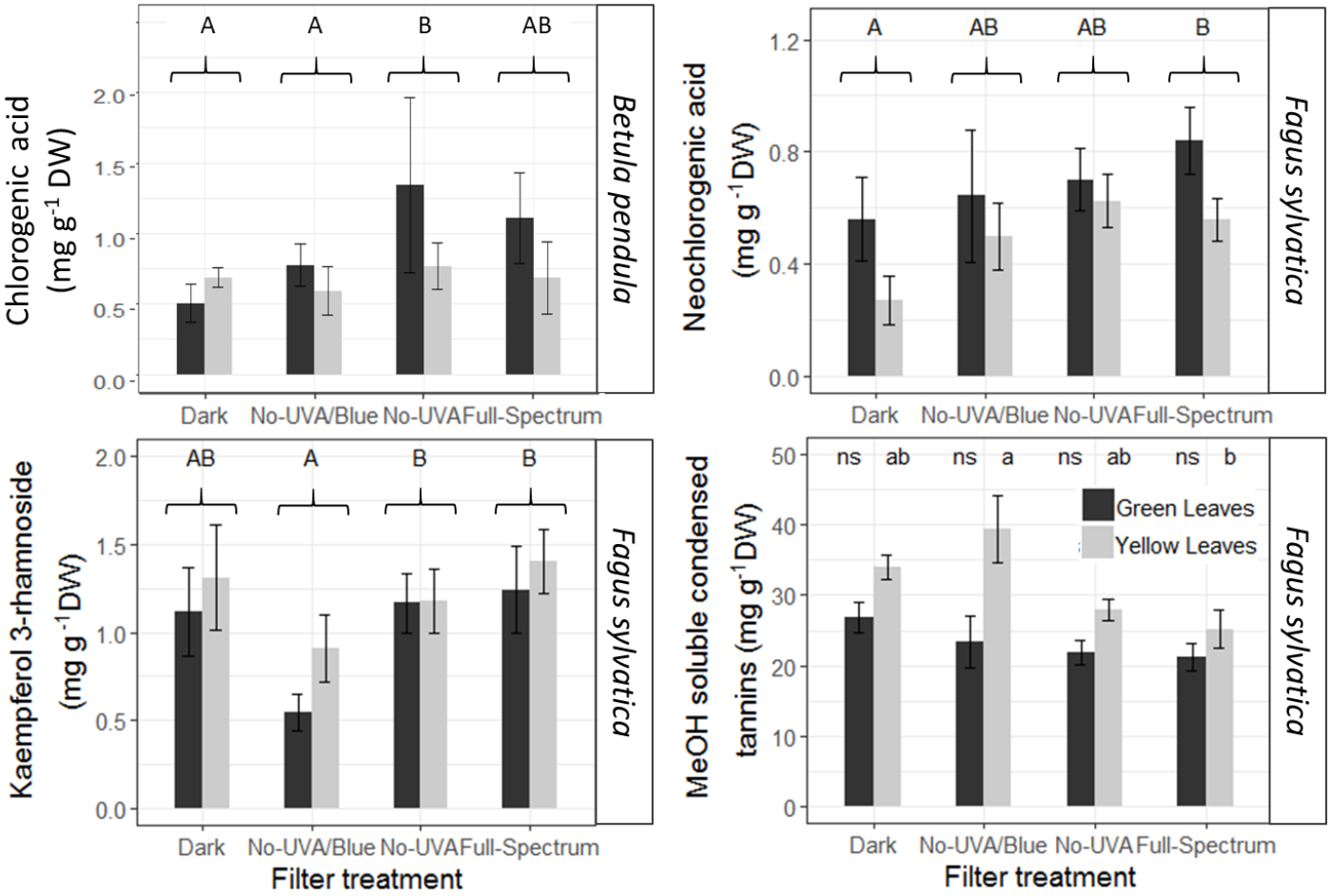

Figure 6: Patterns of leaf phenolics compound composition following the controlled photodegradation experiment, mapped against explanatory variables for each species using nonmetric multidimensional scaling (MDS). *Fagus sylvatica* MDS had a stress of 0.125 and clear segregation according to (A) leaf colour along MDS1 (vs MDS2) and (B) leaf orientation along MDS2 (vs MDS3), but not according to (C) filter treatment. *Betula pendula* MDS had a stress of 0.219, and similar patterns of segregation according to the explanatory variables, (D) leaf colour along MDS1 (vs MDS2) and (E) leaf orientation along MDS2 (vs MDS1).

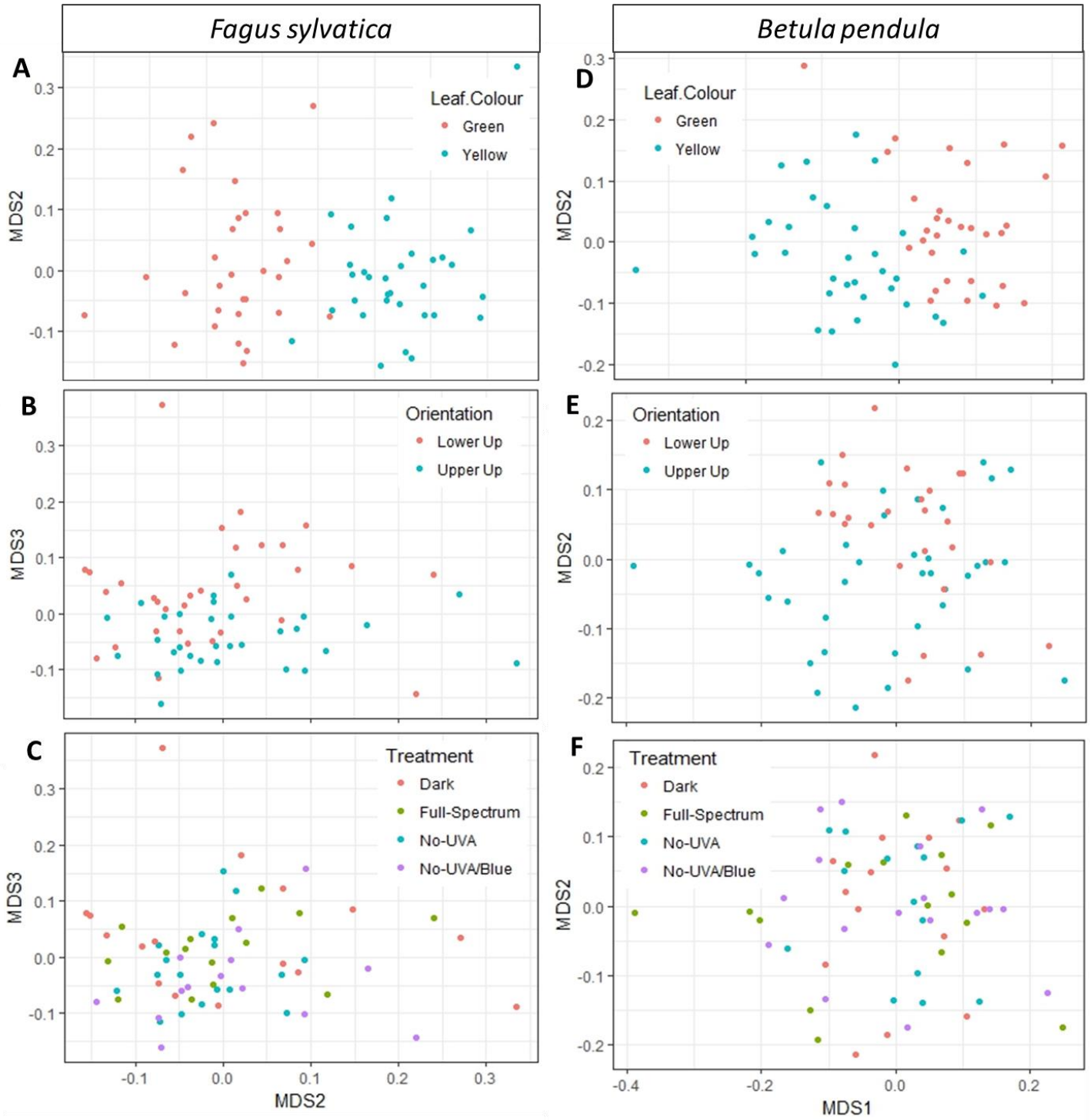

Tables

Table 1: Mean (± 1 SE) values and ANOVA table for average daily mass loss, C and N content and C:N in yellow and green leaves of *F. sylvatica* and *B. pendula* in the controlled photodegradation experiment (up to 77 days). $p < 0.05$ are in bold face, and $0.05 < p < 0.10$ underlined.

Species	***F. sylvatica***		***B. pendula***		**ANOVA**		
Leaf colour	**Green**	**Yellow**	**Green**	**Yellow**	**Colour (C)**	**Species (S)**	**C × S**
Mass Loss (% day^{-1})	0.62 ± 0.02	0.47 ± 0.02	0.66 ± 0.02	0.41 ± 0.02	F = 224 **p = 0.003**	F = 1.04 p = 0.370	F = 17.7 p = 0.052
C content (% g g^{-1})	45.45 ± 0.12	45.41 ± 0.15	48.32 ± 0.11	49.47 ± 0.15	F = 15.8 p = 0.058	F = 665 **p = 0.001**	F = 19.5 **p = 0.048**
N content (% g g^{-1})	2.26 ± 0.03	1.40 ± 0.02	3.01 ± 0.04	1.18 ± 0.03	F = 1581 **p < 0.001**	F = 55.7 **p = 0.017**	F = 204 **p = 0.005**
C:N Ratio	20.38 ± 0.31	32.47 ± 0.41	16.29 ± 0.26	43.61 ± 1.37	F = 882 **p = 0.001**	F = 31.9 **p = 0.030**	F = 135 **p = 0.007**

Species	***F. sylvatica***				**ANOVA**	***B. pendula***				**ANOVA**
Filter Treatment	**Dark**	**No UVA / Blue**	**No UVA**	**Full Spectrum**	**Filter Treatment**	**Dark**	**No UVA / Blue**	**No UVA**	**Full Spectrum**	**Filter Treatments**
Green leaves										
Mass Loss (% day^{-1})	0.58 ± 0.03	0.60 ± 0.02	0.62 ± 0.02	0.68 ± 0.02	F = 2.59 p = 0.062	0.64 ± 0.02	0.65 ± 0.02	0.67 ± 0.02	0.68 ± 0.01	F = 1.49 p = 0.226
C content (% g g^{-1})	45.34±0.41	44.95±0.27	45.36±0.16	45.54±0.20	F = 0.08 p = 0.777	48.58±0.23	47.99± 0.27	47.99±0.23	48.24±0.33	F = 0.38 p = 0.541
N content (% g g^{-1})	2.21 ± 0.06	2.25 ± 0.06	2.30 ± 0.06	2.28 ± 0.07	F = 0.19 p = 0.828	3.00 ± 0.10	3.09 ± 0.09	2.96 ± 0.07	2.91 ± 0.10	F = 0.72 p = 0.484
C:N Ratio	20.77± 0.59	20.28±0.59	19.96±0.61	20.34±0.70	F = 0.10 p = 0.903	16.47±0.61	15.67±0.44	16.30±0.39	16.87±0.65	F = 0.87 p = 0.359
Yellow leaves										
Mass Loss (% day^{-1})	0.46 ± 0.02	0.46 ± 0.03	0.47 ± 0.02	0.47 ± 0.02	F = 0.09 p = 0.965	0.39 ± 0.03	0.40 ± 0.03	0.39 ± 0.02	0.45 ± 0.03	F = 2.31 p = 0.085
C content (% g g^{-1})	45.57±0.32	45.43± 0.36	45.54±0.28	44.91±0.26	F = 1.13 p = 0.332	49.41±0.30	49.94±0.34	49.34±0.35	48.99± 0.24	F = 1.67 p = 0.424
N content (% g g^{-1})	1.41 ± 0.04	1.41 ± 0.04	1.43 ± 0.04	1.39 ± 0.03	F = 0.33 p = 0.719	1.27 ± 0.08	1.16 ± 0.04	1.18 ± 0.07	1.13 ± 0.08	F = 4.71 **p = 0.048**
C:N Ratio	32.64±0.89	32.54±0.85	31.95±0.77	32.45±0.84	F = 0.15 p = 0.869	41.9±2.82	44.74±2.08	43.87±2.13	46.09±2.61	F = 4.15 p = 0.061

793 **Table 2:** Mixed model ANOVA giving overall effects of filter treatments on mass loss, [C], [N], and C:N ratio from the controlled photodegradation experiment.

Response	Dark	No UVA / Blue	No UVA	Full Spectrum	ANOVA Filter Treatments
Controlled Mass Loss (% day^{-1})	0.52 ± 0.02	0.53 ± 0.02	0.54 ± 0.02	0.57 ± 0.02	F = 4.28 ***p* = 0.028**
C content (% g g^{-1})	47.22 ±0.31	47.08 ±0.31	47.06 ±0.25	46.92 ±0.26	F = 0.55 *p* = 0.657
N content (% g g^{-1})	1.97 ± 0.07	1.98 ± 0.06	1.97 ± 0.06	1.93 ± 0.07	F = 0.32 *p* = 0.812
C:N Ratio	27.9 ± 1.2	28.3 ± 1.0	28.0 ± 1.0	28.9 ± 1.2	F = 0.42 *p* = 0.739

794

Table 3: Mean (± 1 SE) rate of mass loss from leaf litter in each stand (up to 186 days). Baseline differences between the stands are exemplified by value from the dark litter bags, and filter treatment effects shown in Fig. 3 as response ratios. ANOVA table for daily mass loss in the forest decomposition experiment for each filter treatment and stand and the interaction between them. $p < 0.05$ are in bold face.

Mass Loss (% day^{-1}) Forest Stands (mean ± 1 SE under dark filter treatment)				
Species	***F. sylvatica* litter**		***B. pendula* litter**	
Leaf colour	**Green**	**Yellow**	**Green**	**Yellow**
Picea abies stand	0.16 ± 0.01	0.10 ± 0.01	0.48 ± 0.01	0.23 ± 0.03
Fagus sylvatica stand	0.16 ± 0.01	0.11 ± 0.01	0.36 ± 0.04	0.17 ± 0.02
Acer platanoides stand	0.14 ± 0.01	0.10 ± 0.01	0.27 ± 0.02	0.18 ± 0.01
Betula pendula stand	0.13 ± 0.01	0.10 ± 0.01	0.29 ± 0.01	0.17 ± 0.01
ANOVA (Forest stands)				
Filter Treatment (F)	F = 1.91 ***p* < 0.001**	F = 4.79 ***p* < 0.001**	F = 4.07 ***p* < 0.001**	F = 0.32 *p* = 0.807
Stand (St)	F = 23.14 ***p* < 0.001**	F = 2.97 ***p* < 0.001**	F = 22.45 ***p* < 0.001**	F = 13.77 ***p* < 0.001**
F x St	F = 0.51 ***p* < 0.001**	F = 1.23 ***p* < 0.001**	F = 2.02 ***p* < 0.001**	F = 1.25 *p* = 0.258
ANOVA				
Colour (C)		**Species (S)**	**C × S**	
F = 317 ***p* = 0.003**		F = 702 ***p* = 0.001**	F = 114 ***p* = 0.009**	

Supplemental Information

Supplemental Figures

Figure S1 The relationship between (A) chlorophyll content and (B & C) epidermal flavonoids for individual fresh vs. dried leaves of each species. The same leaf was measured with Dualex before and after drying. The Dualex measurements of chlorophyll content of fresh and air-dried green leaves of both species were strongly positively correlated (*F. sylvatica* R^2adj =0.70 or *B. pendula* R^2adj = 0.45; Fig. S1), whereas in yellow leaves the relationship was weaker (F. sylvatica R2adj =0.15 or B. pendula R2adj = 0.02 NS; Fig. S1), possibly due in part to less-even pigmentation across the leaf lamina during senescence. Similarly, leaf flavonol readings were consistent between fresh and dry green leaves and to some extent yellow F. sylvatica leaves, but highly variable in yellow B. pendula leaves (Fig. S1). Since the flavonol index is dependent on chlorophyll as a reference, higher variability in the two indices at low values of chlorophyll would be expected.

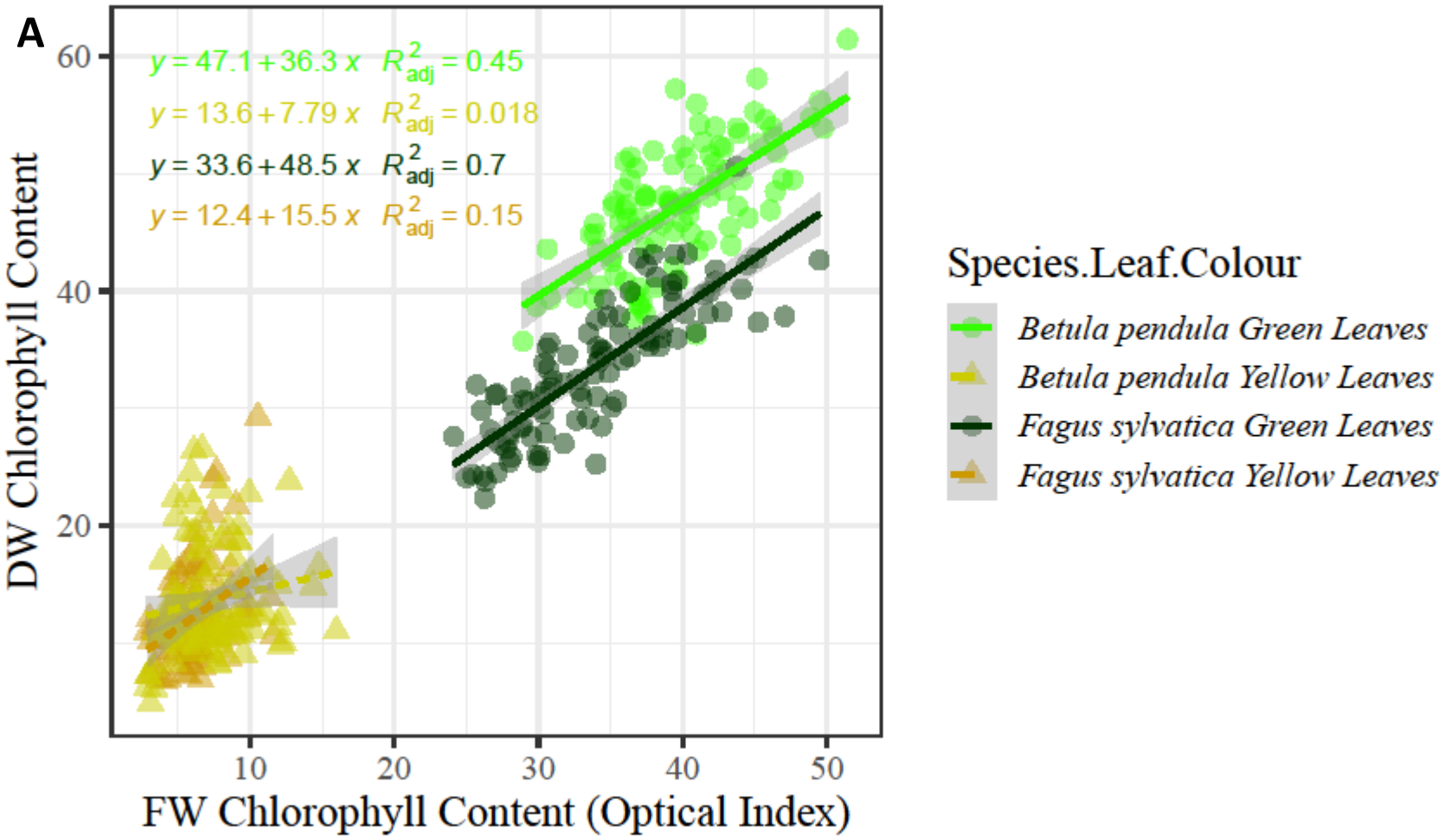

B

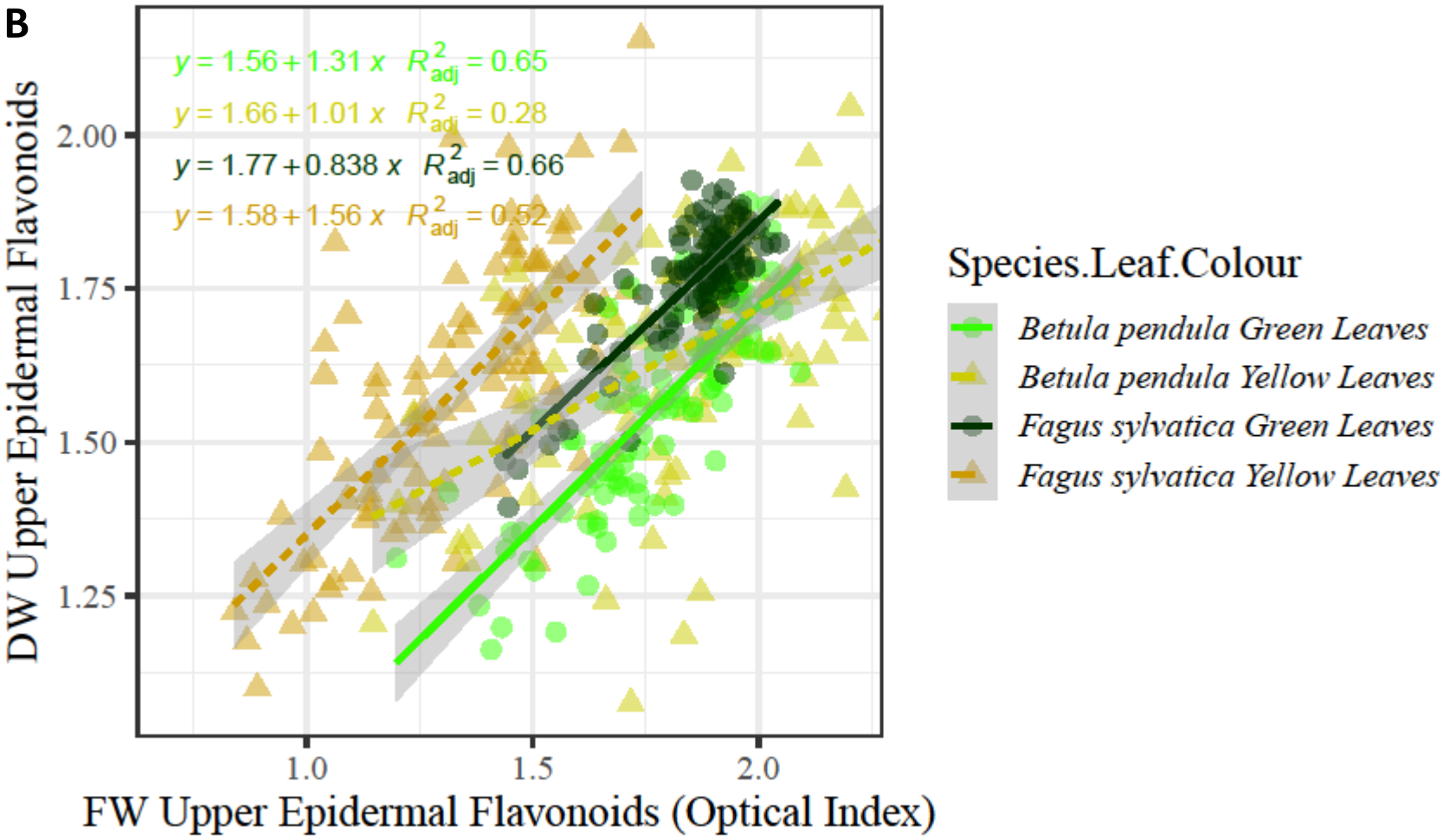
$y = 1.56 + 1.31\,x \quad R^2_{adj} = 0.65$
$y = 1.66 + 1.01\,x \quad R^2_{adj} = 0.28$
$y = 1.77 + 0.838\,x \quad R^2_{adj} = 0.66$
$y = 1.58 + 1.56\,x \quad R^2_{adj} = 0.52$
DW Upper Epidermal Flavonoids
2.00
1.75
1.50
1.25
1.0
1.5
2.0
FW Upper Epidermal Flavonoids (Optical Index)
Species.Leaf.Colour
Betula pendula Green Leaves
Betula pendula Yellow Leaves
Fagus sylvatica Green Leaves
Fagus sylvatica Yellow Leaves

C

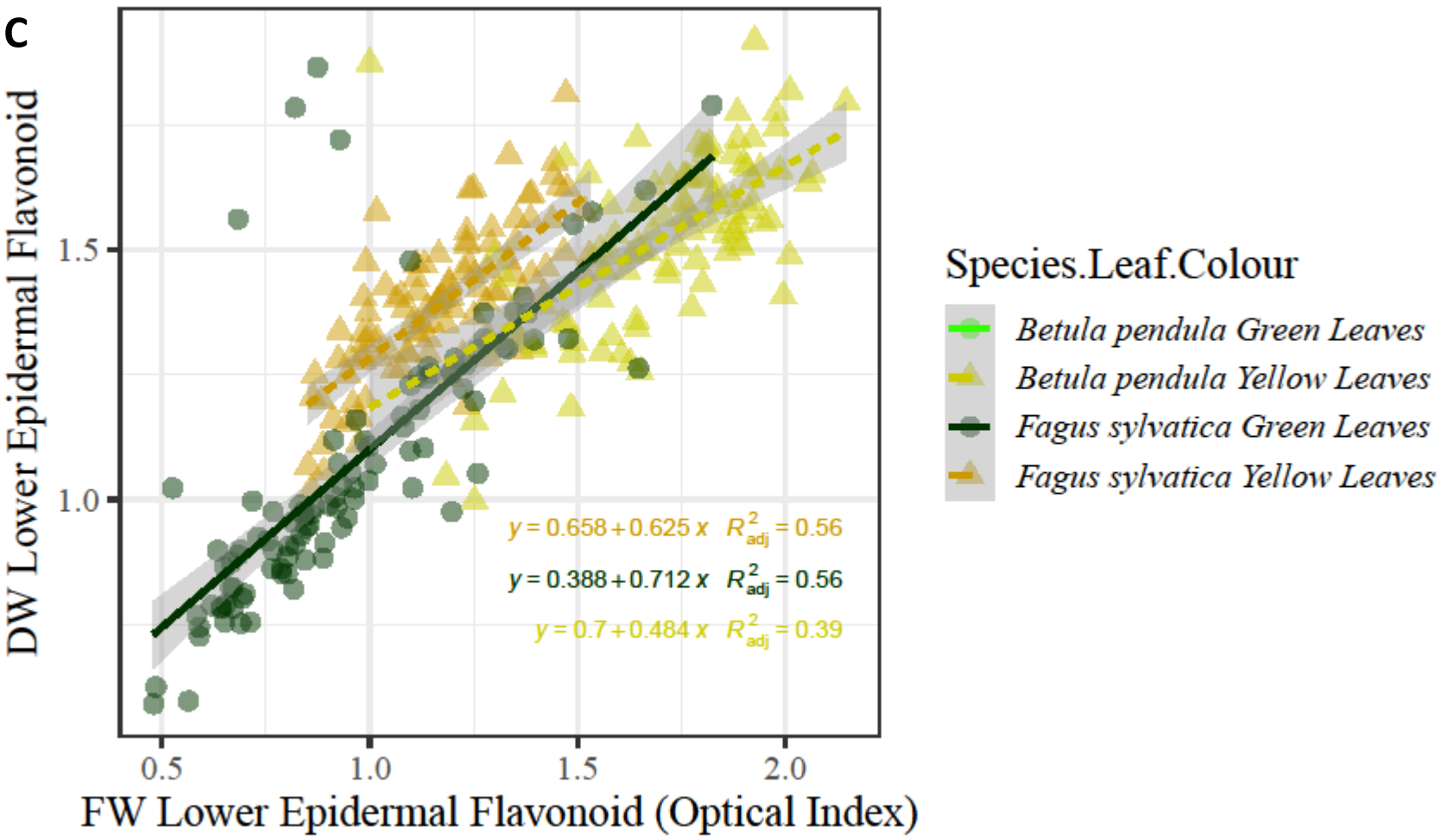

*FW Lower Epidermal Flavonoid data were not collected from *Betula pendula* green leaves.

Figure S2 Scatterplot and linear regressions of the relationship between fresh weight and dry weight of *B. pendula* and *F. sylvatica*, green and yellow leaves. Leaves were weighed before and after drying.

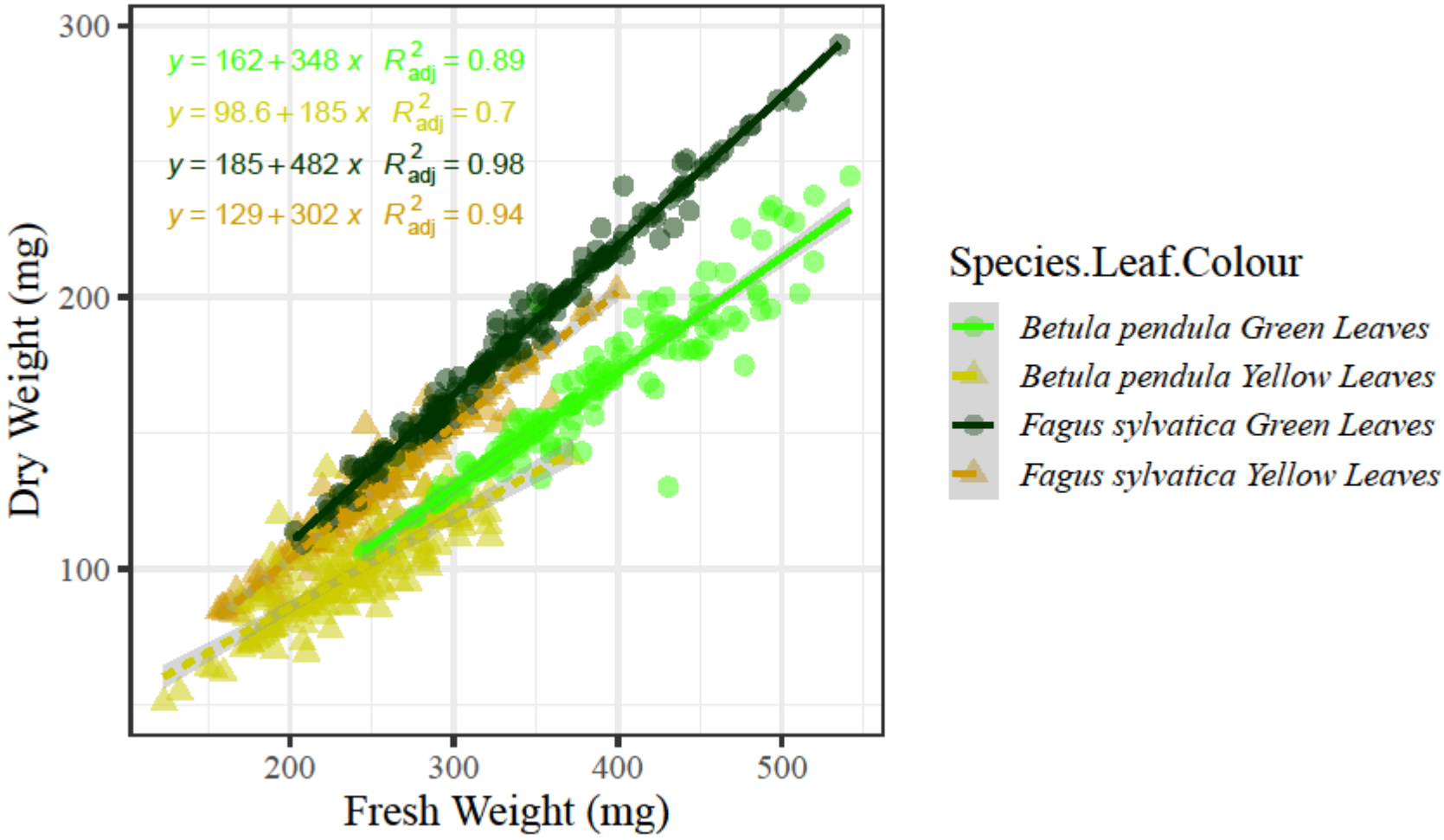

Figure S3 A & B. Arrangement of leaves in the controlled environment experiment, C. in the forest decomposition experiment (*Acer* stand), and D. during installation to show a thin layer of leaf litter from the stand between the net and the soil (*Betula* stand).

Figure S4 Time series of (A) photosynthetically active radiation (PAR), (B) blue light and (C) UV radiation in the stands at Viikki (Helsinki) during the experiment.

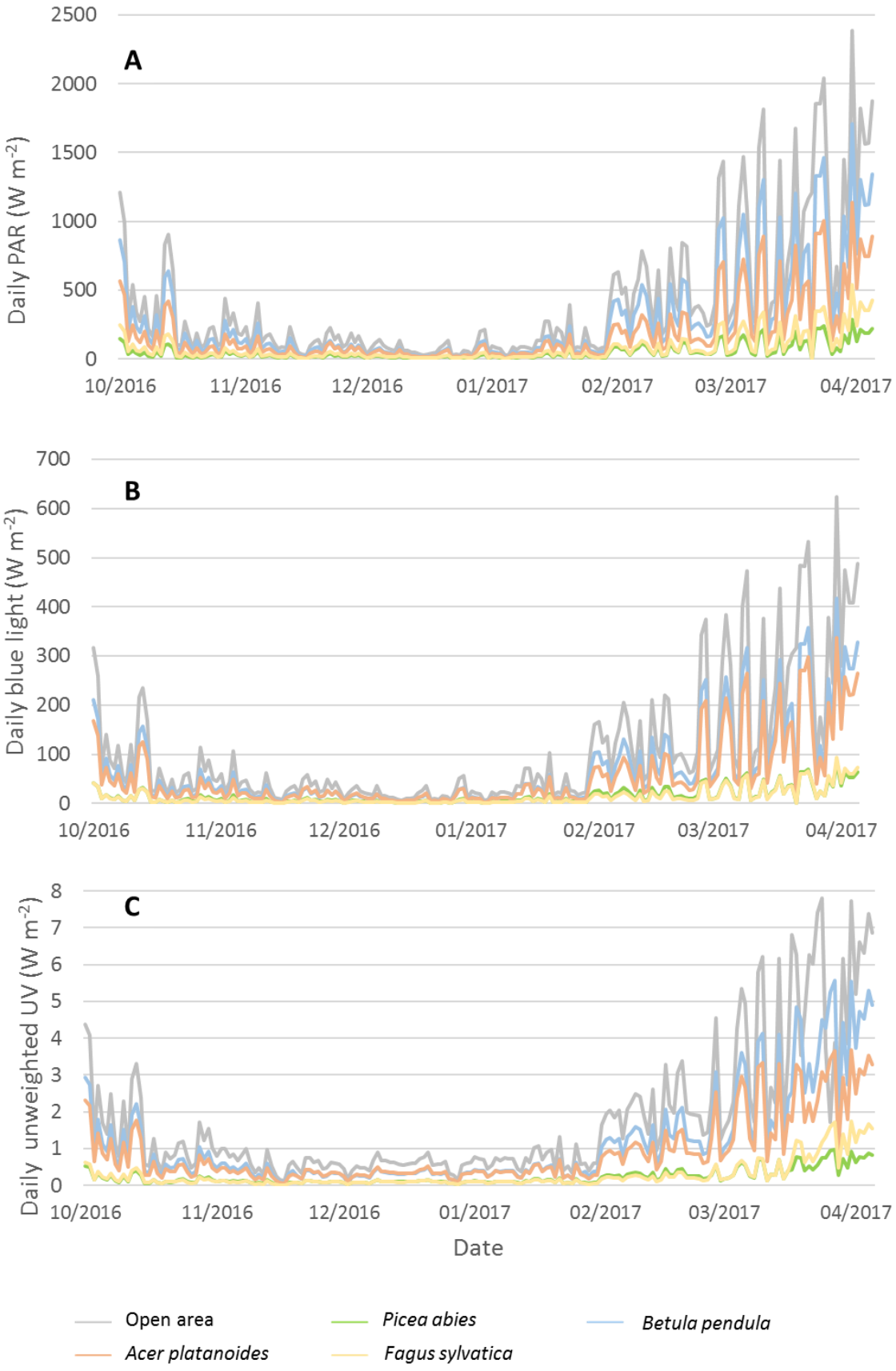

Figure S5 Plot showing average diurnal time courses of (A) leaf surface temperature (red) and relative humidity (blue) in the experimental chamber, and (B) air temperature in different parts of the chamber (centre - orange , side - red, and edge - yellow).

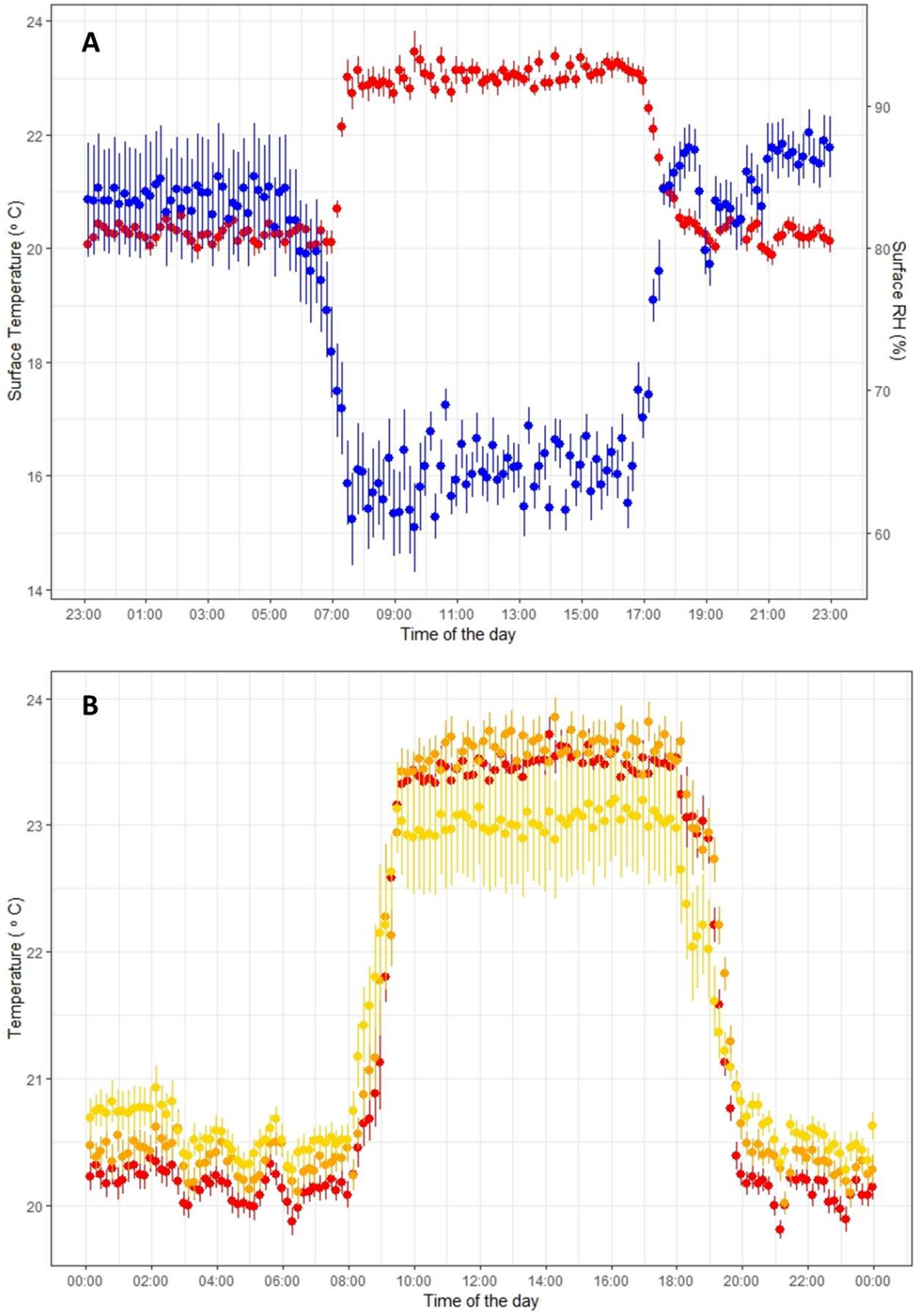

Figure S6 Leaf temperature under controlled conditions according to leaf colour and light exposure treatment. Data measured in the growth room compartments under controlled conditions on 13th October 2016. Leaves under the dark filter are 0.8 °C cooler on average than under the other filters (Effect of Filter $p < 0.001$). Green leaves of silver birch are also 1.0°C cooler on average than the yellow leaves of silver birch and both coloured leaves of beech (Effect of Leaf Colour, $p = 0.001$; Colour x Species $p = 0.005$).

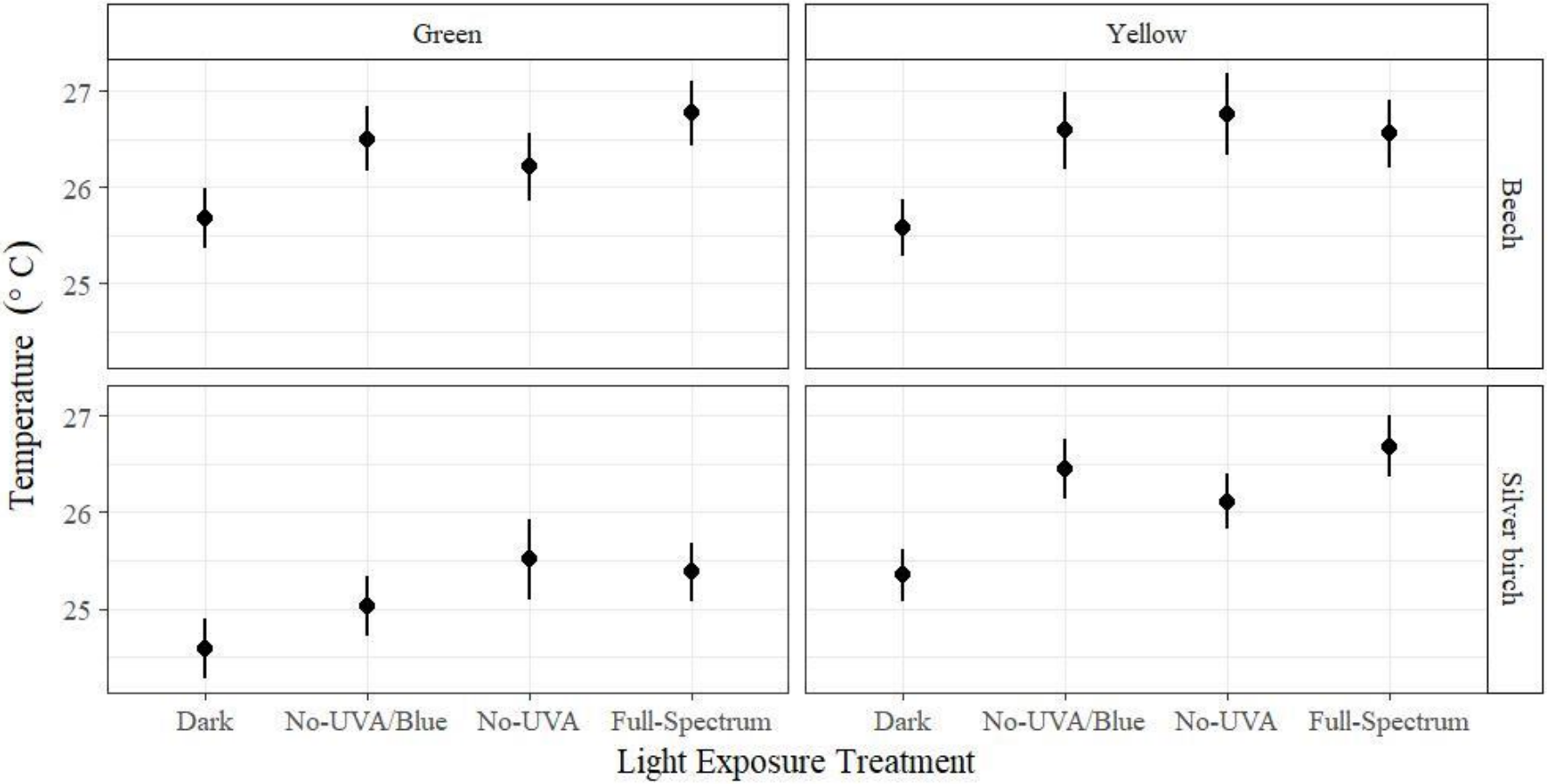

Figure S7 The relationship between epidermal flavonoids for the upper (adaxial) vs. lower (abaxial) epidermis of each species. The same leaf was measured with Dualex on either side.

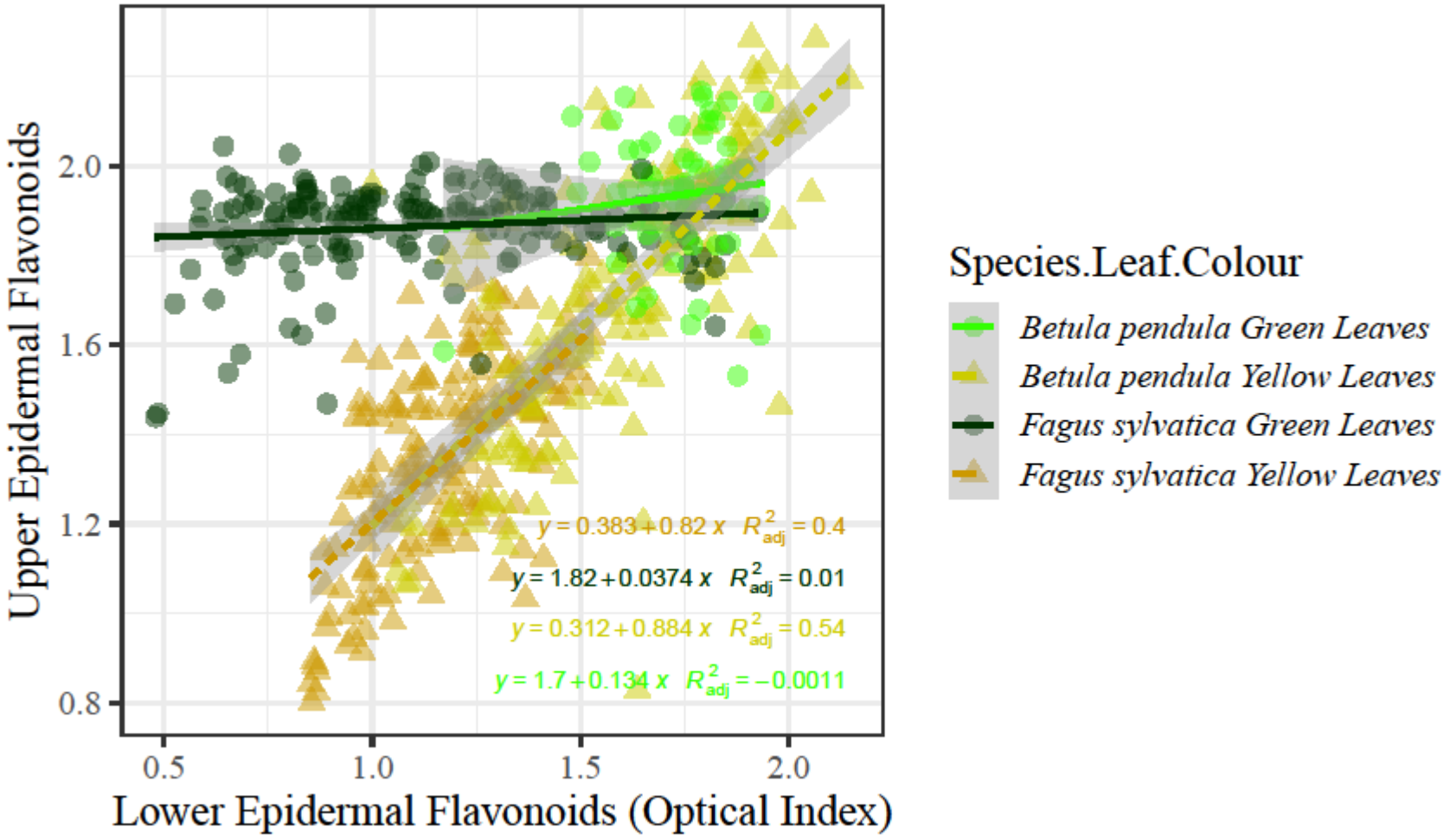

Figure S8 The response ratio of (A) C content and (B) C:N ratio of leaf litter under each filter treatment at the end of the controlled conditions photodegradation experiment. Table 1 gives ANOVA results and means values. Scatterplots of C:N ratio against [N] for leaf from (C) the controlled experiment, and (D) forest stands.

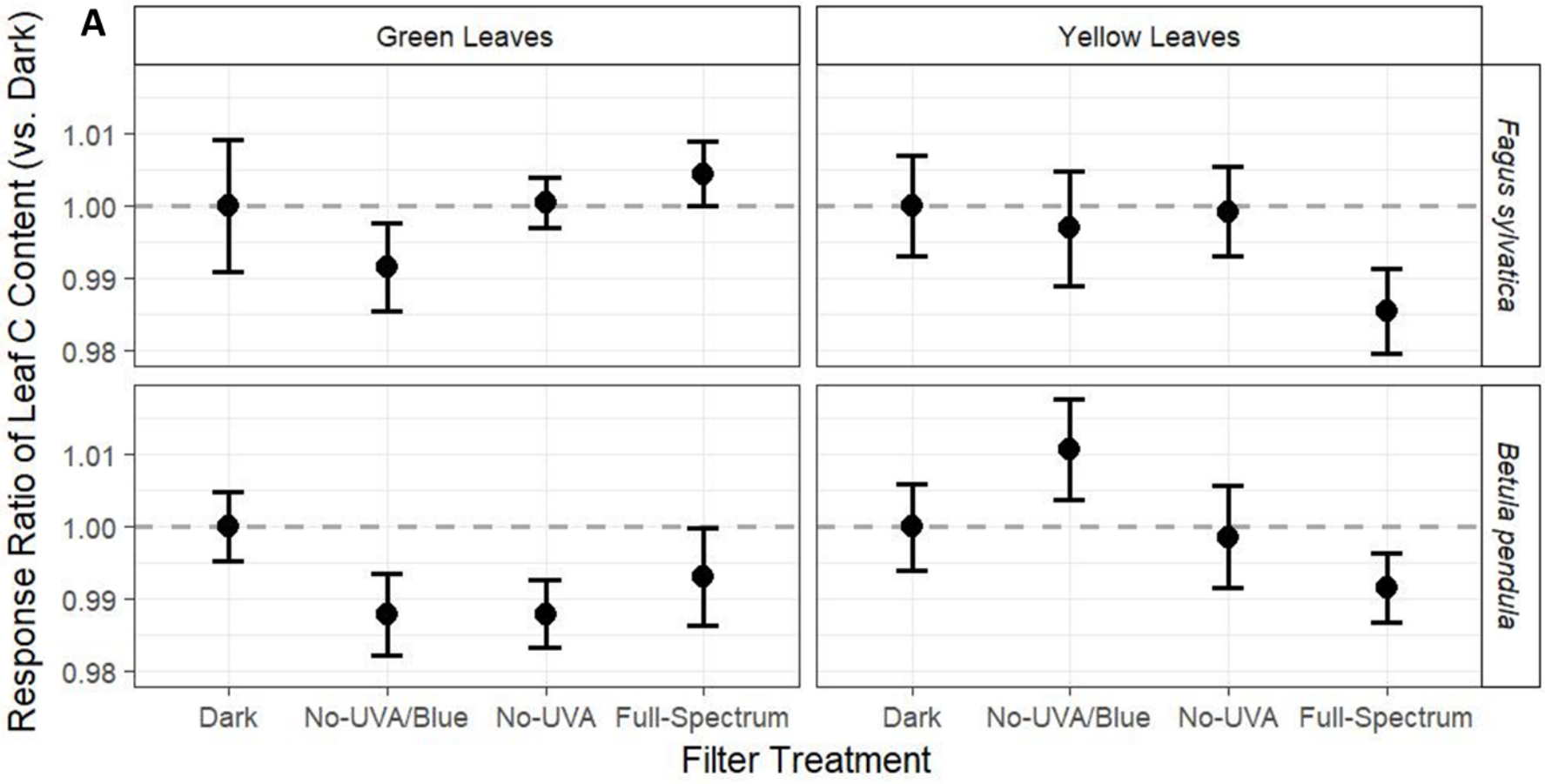

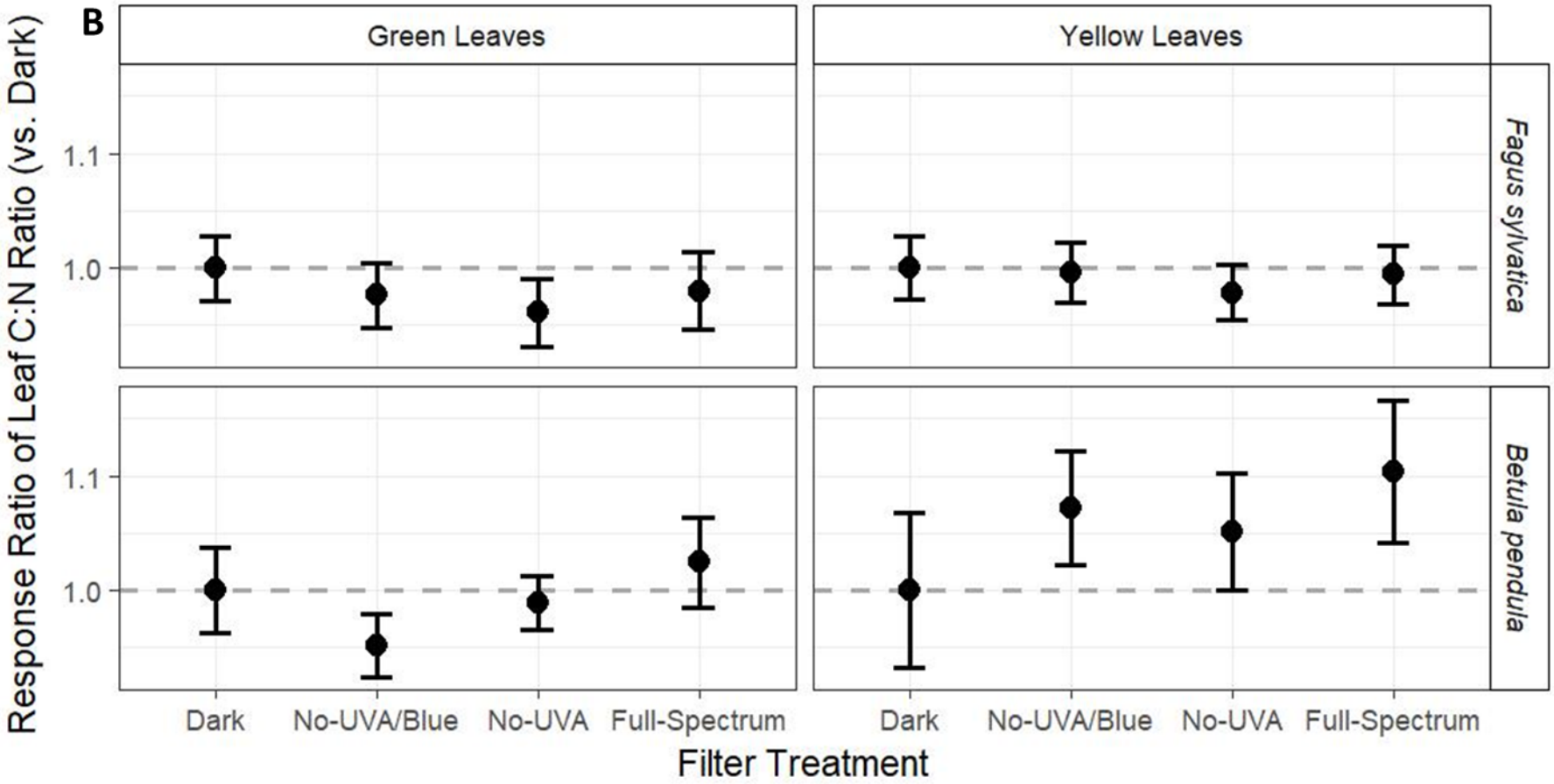
B
Green Leaves
Yellow Leaves
Fagus sylvatica
Betula pendula
Response Ratio of Leaf C:N Ratio (vs. Dark)
1.1
1.0
Dark
No-UVA/Blue
No-UVA
Full-Spectrum
Filter Treatment

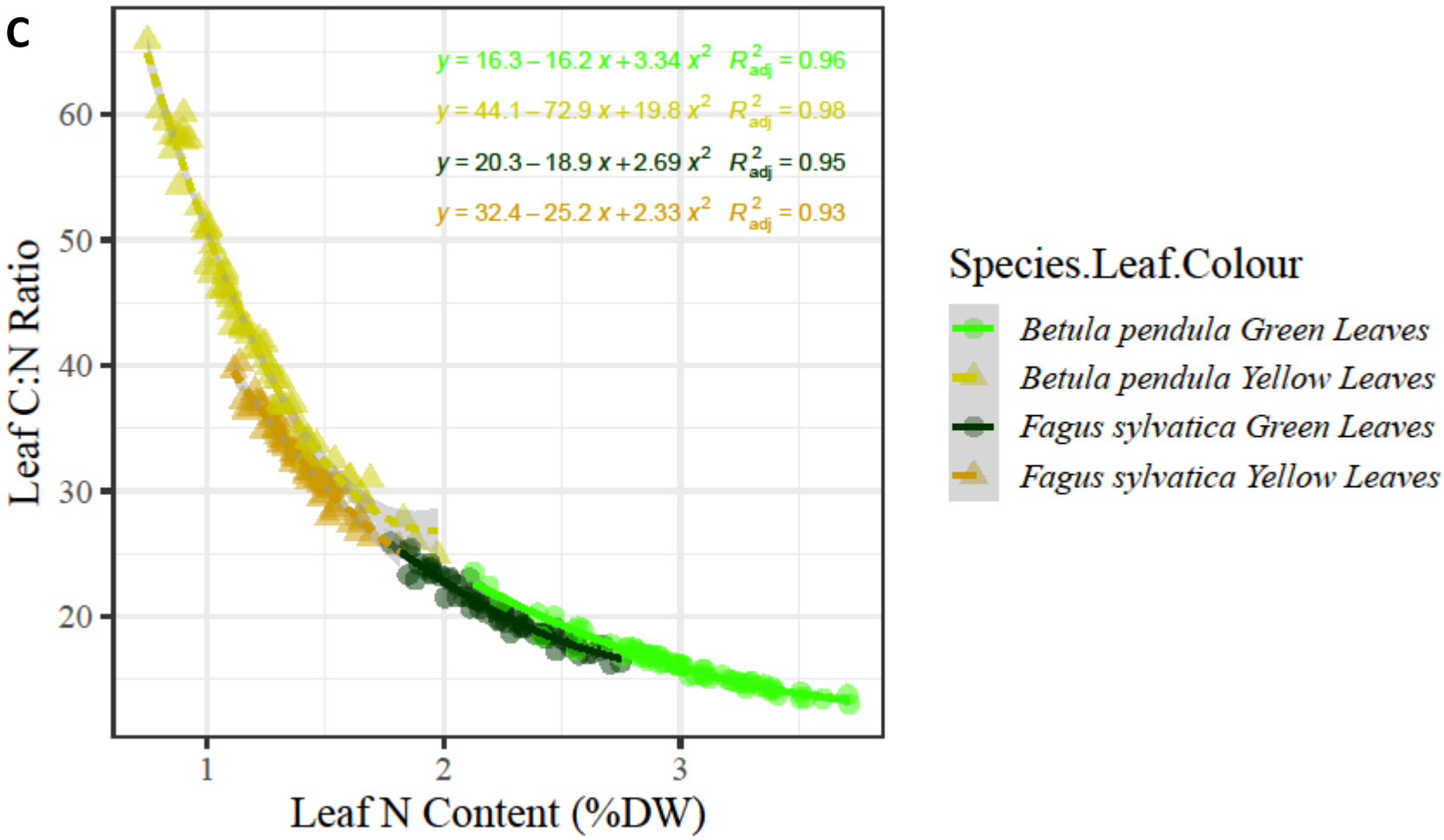

Scatterplot and fitted function of the relationship between leaf nitrogen content (as percentage of dry weight) and leaf carbon/nitrogen ratio of *B. pendula* and *F. sylvatica*, green and yellow leaves after light exposure treatments in controlled conditions for total time of six weeks. Each coloured equation shows corresponding groups' fit and adjusted R^2 value. Leaf phase of senescence is represented either with circle and continuous line (green leaves) or triangle and dotted line (yellow leaves).

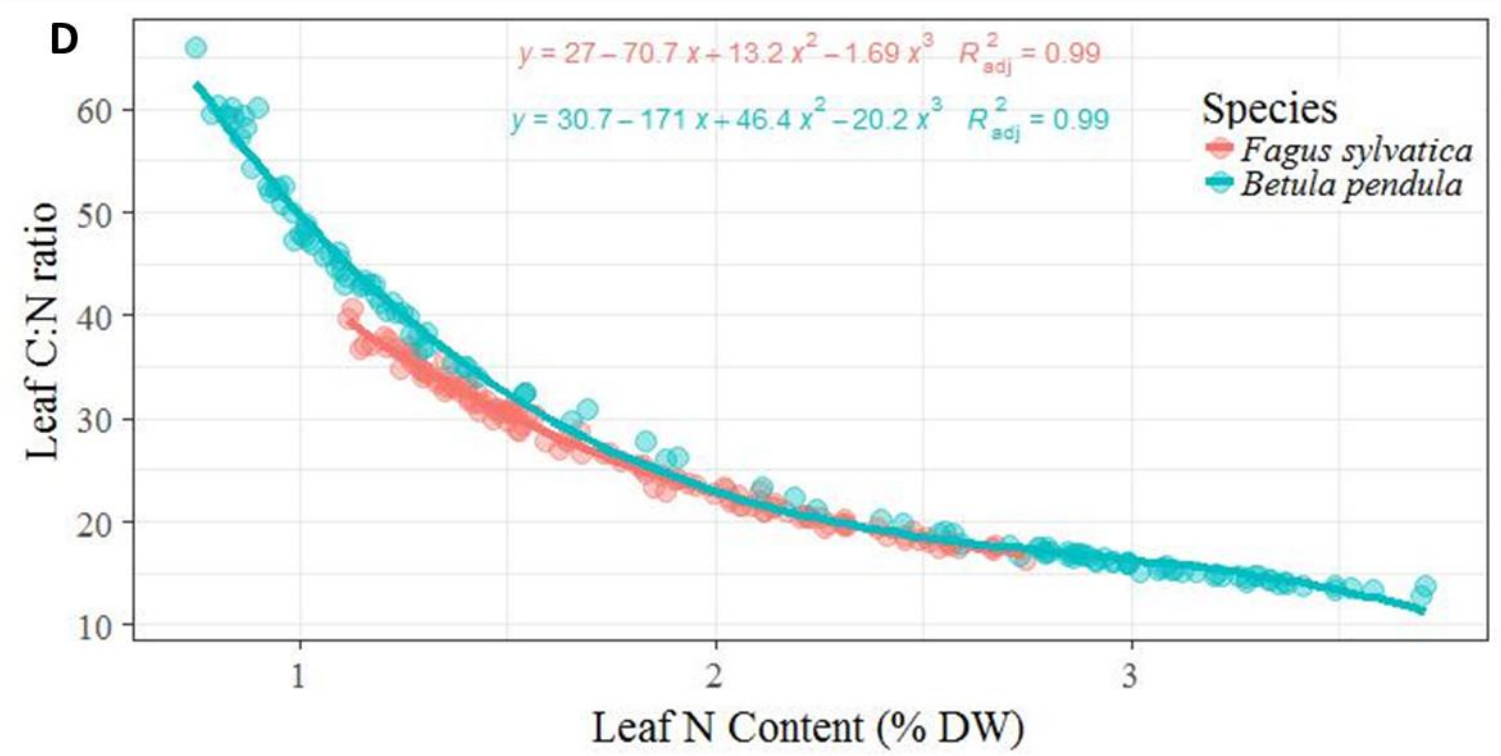

Scatterplot and fitted function of the relationship between leaf nitrogen content (as percentage of dry weight) and leaf carbon/nitrogen ratio of *B. pendula* and *F. sylvatica* leaves that senesced in the stand (collected in December). Each coloured equation shows the fitted function and adjusted R^2 value for the corresponding species. The best fit in each case was to a 3rd order polynomial function. DW- dry weight.

Figure S9 Plot showing daily average temperature (red) ± 1 SE (grey) at the experimental study site in Viikki (Helsinki).

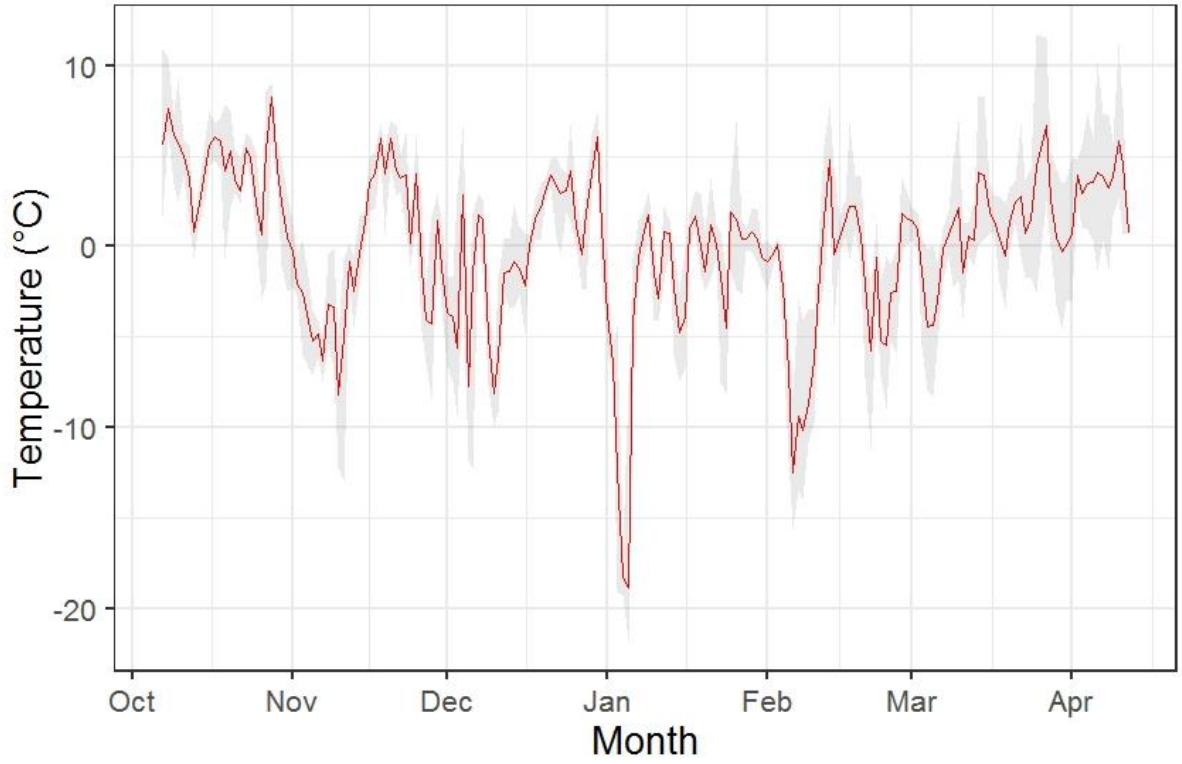

Supplemental Tables

Table S1 The spectral energy irradiance in the controlled experiment growth room under each treatment combination (mean ± SE of measurements from four blocks).

Treatment	PAR	Blue	UV-A
Full Spectrum and UV-A	76.3 ± 1.2 W m^{-2}	13.3 ± 0.2 W m^{-2}	10.19 ± 2.47 W m^{-2}
Full Spectrum No UV-A	74.7 ± 1.2 W m^{-2}	13.0 ± 0.2 W m^{-2}	0.02 ± <0.001 W m^{-2}
No Blue and UV-A	51.8 ± 1.2 W m^{-2}	0.09 ± 0.008 W m^{-2}	12.14 ± 2.49 W m^{-2}
No Blue No UV-A	48.9 ± 1.0 W m^{-2}	0.11 ± W m^{-2}	0.02 ± 0.003 W m^{-2}

Table S2 Examples of the light environment in the forest stands compared with a nearby open area. The mean photon irradiance (µmol m^{-2} s^{-1}) and standard error are shown. Measurements were done using an array spectroradiometer (Maya2000 Pro Ocean Optics, Dunedin, FL, USA; D7-H-SMA cosine diffuser, Bentham Instruments Ltd, Reading, UK) in clear sky conditions on 5th December 2016 at four measuring points in each stand where the leaf litter was placed. R:FR ratio is defined according to Sellaro. Only one measurements was taken in the open where direct sunlight was occluded from the cosine diffusor to create the shade measurement.

Treatment Stand	Position	PAR (PPFD)	Blue	UV-A	UV-B	UV:PAR	B:G	R:FR
Open	Sun	93.9± 0.4	24.6 ± 0.1	11.1 ± 0.1	0.032 ± 0.002	0.119 ± 0.027	1.08 ± 0.01	1.19 ± 0.01
	Shade	69.9	21.9	10.9	0.029	0.156	1.27	1.46
Betula	Sunfleck	64.0 ± 10.3	15.0 ± 1.3	6.4 ± 0.10	0.012 ± 0.001	0.101 ± 0.029	0.99 ± 0.07	1.13 ± 0.01
	Shade	59.6 ± 2.2	14.3 ± 0.1	6.4 ± 0.11	0.017 ± 0.004	0.107 ± 0.011	1.02 ± 0.03	0.89 ± 0.01
Acer	Sunfleck	28.1 ± 0.2	7.5 ± 0.1	3.4 ± 0.10	0.009 ± 0.002	0.122 ± 0.013	1.11 ± 0.01	1.19 ± 0.01
	Shade	25.7 ± 0.9	8.3 ± 0.1	4.2 ± 0.11	0.012 ± 0.003	0.164 ± 0.004	1.30 ± 0.02	1.46 ± 0.03
Fagus	Sunfleck	50.8 ± 11.3	11.4 ± 1.5	5.0 ± 0.10	0.013 ± 0.001	0.099 ± 0.027	0.98 ± 0.08	1.02 ± 0.02
	Shade	31.2 ± 0.8	8.7 ± 0.0	4.5 ± 0.02	0.017 ± 0.001	0.145 ± 0.004	1.20 ± 0.01	1.00 ± 0.01
Picea	Sunfleck	5.4 ± 1.4	1.4 ± 0.2	0.84 ± 0.06	0.061 ± 0.052	0.166 ± 0.080	1.16 ± 0.26	0.94 ± 0.11
	Shade	3.3 ± 0.3	1.0 ± 0.0	0.46 ± 0.03	0.001 ± 0.001	0.141 ± 0.008	1.19 ± 0.01	1.04 ± 0.09

Table S3 Cumulative daily irradiance doses received by the litter at the end of the experiment (6 months) in the forest stands and a nearby open area, under different filter treatments and in unfiltered conditions.

Stand	**Cumulative mean daily Irradiance** Filter treatment /unfiltered	**Photon Irradiance (mol m^{-2})**			**Energy Irradiance (W m^{-2})**		
		UV	**Blue light**	**PAR**	**UV**	**Blue light**	**PAR**
Open	Dark	0.06	0.39	2.02	0.21	20.62	107.47
	No-UV/blue	0.24	4.92	903.21	0.91	261.84	48087.31
	No-UV	32.17	353.70	1370.51	120.11	18831.32	72967.01
	Full-Spectrum	81.91	356.62	1379.85	306.23	18986.74	73464.12
	Unfiltered	*88.58*	*372.32*	*1427.92*	331.18	*19822.76*	*76023.59*
Betula pendula	Dark	0.04	0.25	1.40	0.14	13.08	74.31
	No-UV/blue	0.16	3.18	624.55	0.61	166.03	33251.60
	No-UV	21.34	229.04	947.69	79.68	11940.77	50455.51
	Full-Spectrum	54.31	230.93	954.14	203.02	12039.32	50799.25
	Unfiltered	*58.73*	*241.10*	*987.38*	219.56	*12569.43*	*52569.08*
Acer platanoides	Dark	0.03	0.20	0.93	0.11	10.59	49.69
	No-UV/blue	0.12	2.58	417.64	0.46	134.48	22235.49
	No-UV	16.25	185.58	633.72	60.69	9671.98	33739.83
	Full-Spectrum	41.37	187.11	638.04	154.66	9751.81	33969.69
	Unfiltered	*44.74*	*195.35*	*660.27*	167.26	*10181.20*	*35153.18*
Fagus sylvatica	Dark	0.01	0.05	0.39	0.03	2.60	20.88
	No-UV/blue	0.04	0.63	175.45	0.14	32.96	9341.11
	No-UV	5.05	45.37	266.23	18.86	2370.21	14174.07
	Full-Spectrum	12.87	45.75	268.04	48.12	2389.77	14270.63
	Unfiltered	*13.92*	*47.76*	*277.38*	52.05	*2495.00*	*14767.81*
Picea abies	Dark	0.01	0.05	0.26	0.03	2.86	13.79
	No-UV/blue	0.03	0.69	115.88	0.12	36.29	6169.54
	No-UV	4.20	49.93	175.83	15.67	2610.16	9361.57
	Full-Spectrum	10.61	50.35	177.03	39.90	2631.70	9425.35
	Unfiltered	*11.54*	*52.56*	*183.20*	43.15	*2747.58*	*9753.73*

Table S4 The leaf traits between species and phase of senescence measured prior to the experiment. Irradiance and temperature in each treatment combination (mean ± SE of four compartments). LMA is estimated for leaves used in the experiment from the calibration with the pool of dried leaves. Adaxial Epi refers to the upper epidermis, and abaxial epi the lower epidermis.

Species	***Fagus sylvatica***	***Fagus sylvatica***	***Betula pendula***	***Betula pendula***	ANOVA		
Senescence	**Green**	**Yellow**	**Green**	**Yellow**	**Colour**	**Species**	**Interaction**
Leaf Area (LA cm^2)	21.12 ± 0.33	18.35 ± 0.32	18.36 ± 0.24	16.26 ± 0.32	**F = 375** ***P* = 0.015**	**F = 378** ***P* = 0.015**	F = 1.3 *P* = 0.372
Leaf Fresh Mass Area (LFMA mg cm^{-2})	17.71 ± 0.54	14.85 ± 0.51	18.54 ± 0.43	14.12 ± 0.41	**F = 172** ***P* = 0.006**	F = 0.03 *P* = 0.886	F = 7.93 *P* =0.106
Leaf Mass Area (LMA mg cm^{-2})	9.82 ± 0.26	7.20 ± 0.31	7.44 ± 0.23	5.94 ± 0.21			
Leaf Water Content (g g^{-1})	0.278 ± 0.008	0.132 ± 0.003	0.149 ± 0.008	0.123 ± 0.005	**F = 175** ***P* = 0.006**	**F = 109** ***P* = 0.009**	**F = 85** ***P* = 0.012**
Adaxial Epi Flavonoids (OI)	1.87 ± 0.01	1.38 ± 0.03	1.93 ± 0.02	1.54 ± 0.03	**F = 12.0** ***P* = 0.003**	**F = 22.1** ***P* = 0.042**	F = 4.21 *P* = 0.176
Abaxial Epi Flavonoids (OI)	1.31 ± 0.04	1.19 ± 0.02	1.74 ± 0.01	1.45 ± 0.03	**F = 49.3** ***P* = 0.020**	**F = 162** ***P* = 0.006**	F = 6.44 *P* = 0.126
Chlorophyll Contents (OI)	31.48 ± 0.66	5.64 ± 0.20	35.37 ± 0.53	8.01 ± 0.44	**F = 3238** ***P* < 0.001**	**F = 40.7** ***P* = 0.024**	F = 2.9 *P* = 0.230

Table S5 List of relevant pairwise comparisons for daily mass loss of green and yellow leaves of *Fagus sylvatica* and *Betula pendula* in the forest experiment: t- tests, with the Holm's correction for multiple comparisons, were used to calculate the P values. Significant contrasts are shown in bold.

Fagus sylvatica – green leaves

Stand x Filter treatment (t-value, p-value)

Dark,Picea abies - No-Blue/UV,Picea abies	1.24930529	2.152424e-01
Dark,Picea abies - No-UV,Picea abies	-0.49398333	6.226887e-01
Dark,Picea abies - Full-Spectrum,Picea abies	0.26791392	7.894639e-01
No-Blue/UV,Picea abies - No-UV,Picea abies	-1.74328862	8.517377e-02
No-Blue/UV,Picea abies - Full-Spectrum,Picea abies	-0.98139137	3.293958e-01
No-UV,Picea abies - Full-Spectrum,Picea abies	0.76189724	4.483900e-01
Dark,Fagus sylvatica - No-Blue/UV,Fagus sylvatica	0.21259091	8.321937e-01
Dark,Fagus sylvatica - No-UV,Fagus sylvatica	-0.69640809	4.882173e-01
Dark,Fagus sylvatica - Full-Spectrum,Fagus sylvatica	1.49555538	1.387538e-01
No-Blue/UV,Fagus sylvatica - No-UV,Fagus sylvatica	-0.90899900	3.661155e-01
No-Blue/UV,Fagus sylvatica - Full-Spectrum,Fagus sylvatica	1.28296447	2.032557e-01
No-UV,Fagus sylvatica - Full-Spectrum,Fagus sylvatica	**2.19196347**	**3.132651e-02**
Dark,Acer platanoides - No-Blue/UV,Acer platanoides	0.41194061	6.814986e-01
Dark,Acer platanoides - No-UV,Acer platanoides	-0.12324782	9.022239e-01
Dark,Acer platanoides - Full-Spectrum,Acer platanoides	0.81294549	4.186925e-01
No-Blue/UV,Acer platanoides - No-UV,Acer platanoides	-0.53518843	5.940229e-01
No-Blue/UV,Acer platanoides - Full-Spectrum,Acer platanoides	0.40100488	6.894991e-01
No-UV,Acer platanoides - Full-Spectrum,Acer platanoides	0.93619331	3.520268e-01
Dark,Betula pendula - No-Blue/UV,Betula pendula	0.86312693	3.906805e-01
Dark,Betula pendula - No-UV,Betula pendula	0.09855178	9.217438e-01
Dark,Betula pendula - Full-Spectrum,Betula pendula	0.03605694	9.713279e-01
No-Blue/UV,Betula pendula - No-UV,Betula pendula	-0.76457515	4.468024e-01
No-Blue/UV,Betula pendula - Full-Spectrum,Betula pendula	-0.82706999	4.106886e-01
No-UV,Betula pendula - Full-Spectrum,Betula pendula	-0.06249485	9.503266e-01

Fagus sylvatica – yellow leaves

Stand x Filter treatment (t-value, p-value)

Dark,Picea abies - No-Blue/UV,Picea abies	1.26264965	2.104770e-01
Dark,Picea abies - No-UV,Picea abies	**2.75920256**	**7.217062e-03**
Dark,Picea abies - Full-Spectrum,Picea abies	0.47660336	6.349771e-01
No-Blue/UV,Picea abies - No-UV,Picea abies	1.49655291	1.385452e-01
No-Blue/UV,Picea abies - Full-Spectrum,Picea abies	-0.78604629	4.342218e-01
No-UV,Picea abies - Full-Spectrum,Picea abies	**-2.28259919**	**2.517847e-02**
Dark,Fagus sylvatica - No-Blue/UV,Fagus sylvatica	1.86078307	6.654329e-02
Dark,Fagus sylvatica - No-UV,Fagus sylvatica	**2.82017952**	**6.083044e-03**
Dark,Fagus sylvatica - Full-Spectrum,Fagus sylvatica	**2.40656798**	**1.846848e-02**
No-Blue/UV,Fagus sylvatica - No-UV,Fagus sylvatica	0.95939645	3.403236e-01
No-Blue/UV,Fagus sylvatica - Full-Spectrum,Fagus sylvatica	0.54578491	5.867714e-01
No-UV,Fagus sylvatica - Full-Spectrum,Fagus sylvatica	-0.41361154	6.802936e-01
Dark,Acer platanoides - No-Blue/UV,Acer platanoides	-0.24813209	8.046843e-01
Dark,Acer platanoides - No-UV,Acer platanoides	-0.31972135	7.500344e-01

Dark,Acer platanoides - Full-Spectrum,Acer platanoides	-1.09820665	2.754928e-01
No-Blue/UV,Acer platanoides - No-UV,Acer platanoides	-0.08324621	9.338690e-01
No-Blue/UV,Acer platanoides - Full-Spectrum,Acer platanoides	-0.85007457	3.978855e-01
No-UV,Acer platanoides - Full-Spectrum,Acer platanoides	-0.72689288	4.694676e-01

Dark,Betula pendula - No-Blue/UV,Betula pendula	1.54454363	1.265044e-01
Dark,Betula pendula - No-UV,Betula pendula	1.82655375	7.159287e-02
Dark,Betula pendula - Full-Spectrum,Betula pendula	-0.25172631	8.019147e-01
No-Blue/UV,Betula pendula - No-UV,Betula pendula	0.28201011	7.786827e-01
No-Blue/UV,Betula pendula - Full-Spectrum,Betula pendula	-1.79626994	7.632351e-02
No-UV,Betula pendula - Full-Spectrum,Betula pendula	**-2.07828006**	**4.097235e-02**

Betula pendula – green leaves

Stand x Filter treatment (t-value, p-value)

Dark,Picea abies - No-Blue/UV,Picea abies	1.67299895	9.879132e-02
Dark,Picea abies - No-UV,Picea abies	**2.91698599**	**4.746742e-03**
Dark,Picea abies - Full-Spectrum,Picea abies	**2.49144685**	**1.509522e-02**
No-Blue/UV,Picea abies - No-UV,Picea abies	1.24398704	2.176540e-01
No-Blue/UV,Picea abies - Full-Spectrum,Picea abies	0.81844790	4.158790e-01
No-UV,Picea abies - Full-Spectrum,Picea abies	-0.42553914	6.717492e-01

Dark,Fagus sylvatica - No-Blue/UV,Fagus sylvatica	-0.56665471	5.727613e-01
Dark,Fagus sylvatica - No-UV,Fagus sylvatica	**2.22376770**	**2.939263e-02**
Dark,Fagus sylvatica - Full-Spectrum,Fagus sylvatica	1.40955961	1.630972e-01
No-Blue/UV,Fagus sylvatica - No-UV,Fagus sylvatica	**2.55256242**	**1.287703e-02**
No-Blue/UV,Fagus sylvatica - Full-Spectrum,Fagus sylvatica	1.82740315	7.190158e-02
No-UV,Fagus sylvatica - Full-Spectrum,Fagus sylvatica	-0.88039355	3.816588e-01

Dark,Acer platanoides - No-Blue/UV,Acer platanoides	0.11758821	9.067307e-01
Dark,Acer platanoides - No-UV,Acer platanoides	0.37922330	7.056700e-01
Dark,Acer platanoides - Full-Spectrum,Acer platanoides	0.18980308	8.500128e-01
No-Blue/UV,Acer platanoides - No-UV,Acer platanoides	0.26163508	7.943711e-01
No-Blue/UV,Acer platanoides - Full-Spectrum,Acer platanoides	0.07221486	9.426369e-01
No-UV,Acer platanoides - Full-Spectrum,Acer platanoides	-0.18942022	8.503116e-01

Dark,Betula pendula - No-Blue/UV,Betula pendula	**-2.55463288**	**1.280733e-02**
Dark,Betula pendula - No-UV,Betula pendula	-1.46579052	1.471831e-01
Dark,Betula pendula - Full-Spectrum,Betula pendula	0.27198974	7.864305e-01
No-Blue/UV,Betula pendula - No-UV,Betula pendula	1.15426290	2.523179e-01
No-Blue/UV,Betula pendula - Full-Spectrum,Betula pendula	**2.86922806**	**5.435928e-03**
No-UV,Betula pendula - Full-Spectrum,Betula pendula	1.77909839	7.956495e-02

Table S6 Phenolic compounds isolated from leaf litter of *B. pendula* and *F. sylvatica* by HLPC follow the controlled-conditions experiment. Each point shows mean ± SE expressed in mg g^{-1} DW.

Fagus sylvatica	Green leaves								Yellow leaves							
	Adaxial up				Abaxial up				Adaxial up				Abaxial up			
	Dark	No-UVA/ Blue	No-UVA	Full-spectrum	Dark	No-UVA/ Blue	No-UVA	Full-spectrum	Dark	No-UVA/ Blue	No-UVA	Full-spectrum	Dark	No-UVA/ Blue	No-UVA	Full-spectrum
STILBENES																
Taxifolin xyloside	0.94 ± 0.04	0.85 ± 0.19	0.98 ± 0.26	0.90 ± 0.15	1.28 ± 0.31	1.21 ± 1.05	1.13 ± 0.33	1.16 ± 0.25	0.99 ± 0.28	0.54 ± 0.14	0.81 ± 0.42	1.66 ± 0.58	0.56 ± 0.08	0.92 ± 0.19	0.60 ± 0.03	0.58 ± 0.13
Taxifolin glucoside	1.17 ± 0.35	0.95 ± 0.21	0.90 ± 0.20	0.62 ± 0.32	0.91 ± 0.16	0.61 ± 0.41	0.96 ± 0.26	0.99 ± 0.31	0.88 ± 0.20	0.88 ± 0.20	1.23 ± 0.42	1.35 ± 0.42	1.19 ± 0.04	1.37 ± 0.29	1.47 ± 0.14	1.30 ± 0.24
Taxifolin aglycon	1.83 ± 0.88	0.75 ± 0.16	0.96 ± 0.37	0.59 ± 0.17	0.68 ± 0.09	0.46 ± 0.46	0.18 ± 0.22	0.46 ± 0.23	0.80 ± 0.06	0.71 ± 0.24	1.11 ± 0.22	0.97 ± 0.13	0.90 ± 0.05	1.12 ± 0.37	1.09 ± 0.08	1.12 ± 0.16
Sum, stilbenes	*3.94 ± 1.20*	*2.56 ± 0.37*	*2.85 ± 0.74*	*2.11 ± 0.07*	*2.88 ± 0.37*	*2.28 ± 1.93*	*3.26 ± 0.71*	*3.57 ± 0.95*	*2.67 ± 0.38*	*2.47 ± 0.75*	*3.27 ± 0.97*	*3.86 ± 0.66*	*2.64 ± 0.13*	*3.40 ± 0.76*	*3.16 ± 0.10*	*3.00 ± 0.48*
FLAVONOIDS																
Myricetin 3-rhamnoside	0.72 ± 0.19	0.53 ± 0.31	1.29 ± 0.40	1.12 ± 0.21	0.59 ± 0.24	0.56 ± 0.08	0.79 ± 0.19	1.14 ± 0.17	1.08 ± 0.15	0.80 ± 0.41	1.32 ± 0.40	1.40 ± 0.34	1.66 ± 0.08	1.76 ± 0.32	1.51 ± 0.08	1.59 ± 0.31
Quercetin 3-rhamnoside	12.38 ± 2.23	13.40 ± 2.31	14.79 ± 1.87	15.76 ± 0.64	10.46 ± 2.80	7.72 ± 0.52	9.88 ± 2.19	7.54 ± 0.60	20.61 ± 3.68	14.68 ± 4.63	16.90 ± 3.49	21.63 ± 4.44	22.37 ± 5.03	15.07 ± 1.26	18.25 ± 5.39	17.80 ± 5.53
Quercetin 3-galactoside	10.54 ± 3.47	11.84 ± 2.69	12.37 ± 2.24	13.04 ± 2.05	9.34 ± 1.53	7.76 ± 5.30	9.23 ± 2.31	8.56 ± 1.30	14.44 ± 3.43	11.00 ± 1.92	11.23 ± 2.03	15.03 ± 4.97	19.62 ± 3.24	11.40 ± 0.85	20.03 ± 6.47	15.17 ± 3.54
Quercetin 3-glucoside	4.70 ± 1.70	4.98 ± 1.34	5.16 ± 1.10	5.59 ± 1.25	2.73 ± 0.46	1.65 ± 0.74	4.19 ± 0.94	1.81 ± 0.42	6.52 ± 1.06	5.60 ± 0.64	4.51 ± 0.61	8.16 ± 2.26	7.28 ± 2.04	4.21 ± 0.43	5.08 ± 0.72	6.31 ± 1.14
Quercetin 7-glycoside	0.35 ± 0.35	0.10 ± 0.10	0.25 ± 0.15	0.24 ± 0.24	0.72 ± 0.11	0.27 ± 0.01	0.53 ± 0.21	0.59 ± 0.28	0.82 ± 0.25	0.82 ± 0.18	0.23 ± 0.15	0.91 ± 0.46	0.96 ± 0.22	0.45 ± 0.26	1.01 ± 0.35	1.15 ± 0.49
Kaempferol 3-galactoside	4.57 ± 1.24	3.72 ± 0.63	4.09 ± 0.28	4.10 ± 0.64	3.23 ± 0.43	1.78 ± 0.99	3.46 ± 0.59	2.76 ± 0.44	3.85 ± 0.90	3.78 ± 0.56	3.63 ± 0.18	4.67 ± 1.73	4.50 ± 1.42	3.70 ± 0.52	4.56 ± 0.63	4.91 ± 1.13
Kaempferol 3-glucoside	11.49 ± 4.24	9.25 ± 1.43	10.42 ± 1.76	10.80 ± 2.98	14.87 ± 1.97	15.86 ± 3.05	11.03 ± 2.12	12.57 ± 3.87	9.72 ± 1.40	9.61 ± 1.64	9.09 ± 1.95	12.49 ± 0.47	18.15 ± 3.00	9.58 ± 2.05	11.38 ± 2.78	12.16 ± 1.10
Kaempferol 3-arabinoside	3.62 ± 0.47	3.47 ± 0.47	3.64 ± 0.13	4.49 ± 1.54	2.92 ± 0.76	1.80 ± 1.31	2.89 ± 0.54	2.47 ± 0.34	4.53 ± 0.39	4.38 ± 0.30	3.50 ± 0.55	5.51 ± 0.58	4.33 ± 1.00	3.33 ± 0.37	4.02 ± 0.18	4.67 ± 0.45
Kaempferol 3-rhamnoside	1.26 ± 0.62	0.65 ± 0.12	0.97 ± 0.22	1.23 ± 0.44	1.07 ± 0.30	0.32 ± 0.09	1.36 ± 0.25	1.25 ± 0.34	0.77 ± 0.18	0.86 ± 0.41	0.89 ± 0.17	1.17 ± 0.32	2.22 ± 0.25	0.96 ± 0.05	1.66 ± 0.15	1.55 ± 0.21
Monocoumaroyl-astragallin 1	0.28 ± 0.28	0.35 ± 0.21	0.53 ± 0.27	0.30 ± 0.15	-	0.33 ± 0.33	0.11 ± 0.11	0.06 ± 0.06	-	-	-	-	-	-	-	-
Monocoumaroyl-astragallin 2	0.65 ± 0.18	0.51 ± 0.27	0.77 ± 0.28	0.47 ± 0.07	0.41 ± 0.25	0.17 ± 0.17	0.23 ± 0.10	0.45 ± 0.28	1.03 ± 0.41	0.87 ± 0.15	0.83 ± 0.55	2.31 ± 0.57	1.19 ± 0.04	0.87 ± 0.10	1.05 ± 0.33	0.83 ± 0.34
Monocoumaroyl-astragallin 3	0.40 ± 0.03	0.15 ± 0.09	0.53 ± 0.32	0.28 ± 0.05	0.29 ± 0.18	0.46 ± 0.46	0.19 ± 0.13	0.37 ± 0.16	1.38 ± 0.22	1.28 ± 0.30	0.80 ± 0.22	1.34 ± 0.12	1.04 ± 0.06	1.07 ± 0.16	1.14 ± 0.30	0.84 ± 0.20
Monocoumaroyl-astragallin 4	0.11 ± 0.11	0.29 ± 0.15	0.65 ± 0.23	0.46 ± 0.23	0.31 ± 0.16	0.21 ± 0.11	0.39 ± 0.12	0.41 ± 0.17	1.08 ± 0.23	0.93 ± 0.20	0.64 ± 0.21	2.08 ± 0.01	0.64 ± 0.64	0.50 ± 0.17	1.62 ± 0.38	0.52 ± 0.26
Dicoumaroyl-astragallin 1	0.10 ± 0.10	0.18 ± 0.13	0.23 ± 0.10	0.19 ± 0.10	0.21 ± 0.13	0.20 ± 0.12	0.34 ± 0.05	0.17 ± 0.14	0.57 ± 0.12	0.67 ± 0.16	0.41 ± 0.18	0.96 ± 0.25	0.93 ± 0.22	0.39 ± 0.30	0.69 ± 0.27	0.44 ± 0.29

Dicoumaroyl-astragallin 2	0.20 ± 0.20	0.06 ± 0.06	0.21 ± 0.14	0.17 ± 0.17	0.11 ± 0.08	0.26 ± 0.26	0.14 ± 0.14	0.14 ± 0.14	0.44 ± 0.11	0.44 ± 0.14	0.14 ± 0.04	0.76 ± 0.36	0.92 ± 0.10	0.23 ± 0.08	0.69 ± 0.35	0.59 ± 0.22
Sum, flavonoids	*51.40 ± 0.74*	*49.51 ± 6.95*	*55.92 ± 5.71*	*58.24 ± 8.31*	*47.28 ± 4.17*	*39.37 ± 13.37*	*44.76 ± 6.68*	*40.32 ± 7.57*	*66.86 ± 8.55*	*55.73 ± 8.10*	*54.15 ± 6.38*	*78.43 ± 13.19*	*85.83 ± 10.63*	*53.55 ± 3.68*	*73.41 ± 18.12*	*68.53 ± 12.50*
PHENOLIC ACIDS																
Hydroxycinnamic acid (HCA)	0.86 ± 0.21	0.51 ± 0.26	0.51 ± 0.11	0.57 ± 0.22	1.15 ± 0.25	0.96 ± 0.77	0.63 ± 0.23	1.39 ± 0.43	0.68 ± 0.22	0.53 ± 0.20	1.03 ± 0.30	0.49 ± 0.20	0.49 ± 0.18	0.41 ± 0.11	0.84 ± 0.19	0.95 ± 0.22
Neochlorogenic acid	0.38 ± 0.13	0.83 ± 0.31	0.89 ± 0.14	0.75 ± 0.07	0.62 ± 0.19	0.27 ± 0.22	0.50 ± 0.13	0.90 ± 0.21	0.31 ± 0.14	0.52 ± 0.21	0.72 ± 0.13	0.48 ± 0.15	0.21 ± 0.04	0.47 ± 0.15	0.47 ± 0.05	0.61 ± 0.09
Chlorogenic acid	3.25 ± 3.00	1.42 ± 0.46	1.26 ± 0.42	1.32 ± 0.43	11.24 ± 3.45	12.39 ± 11.42	7.82 ± 3.87	10.46 ± 3.87	1.97 ± 0.32	1.87 ± 0.62	1.90 ± 0.40	2.50 ± 0.36	1.72 ± 0.33	2.58 ± 0.92	3.99 ± 0.80	2.66 ± 0.72
Chlorogenic acid derivative 1	3.57 ± 0.22	4.28 ± 1.48	2.98 ± 0.94	4.89 ± 2.57	1.73 ± 0.40	1.25 ± 1.25	1.39 ± 0.64	2.01 ± 1.04	0.30 ± 0.05	0.21 ± 0.07	0.51 ± 0.15	0.71 ± 0.43	1.97 ± 0.26	0.27 ± 0.11	0.62 ± 0.39	0.46 ± 0.19
Chlorogenic acid derivative 2	0.12 ± 0.12	0.18 ± 0.08	0.37 ± 0.07	0.34 ± 0.03	0.22 ± 0.04	0.21 ± 0.10	0.22 ± 0.07	0.23 ± 0.08	0.54 ± 0.02	0.47 ± 0.13	0.52 ± 0.13	0.59 ± 0.05	0.55 ± 0.04	0.61 ± 0.02	0.63 ± 0.05	0.54 ± 0.12
Chlorogenic acid derivative 3	0.45 ± 0.12	0.36 ± 0.12	0.44 ± 0.10	0.47 ± 0.14	0.28 ± 0.07	0.23 ± 0.10	0.39 ± 0.08	0.44 ± 0.06	0.62 ± 0.78	0.78 ± 0.17	0.58 ± 0.07	0.61 ± 0.18	0.87 ± 0.03	0.74 ± 0.01	0.89 ± 0.13	0.64 ± 0.13
Chlorogenic acid derivative 4	0.43 ± 0.04	0.37 ± 0.13	0.46 ± 0.08	0.48 ± 0.08	0.27 ± 0.06	0.25 ± 0.05	0.26 ± 0.05	0.36 ± 0.11	0.47 ± 0.11	0.23 ± 0.08	0.43 ± 0.17	0.68 ± 0.14	-	0.38 ± 0.22	0.19 ± 0.19	0.28 ± 0.20
Chlorogenic acid derivative 5	0.41 ± 0.11	0.28 ± 0.05	0.27 ± 0.03	0.11 ± 0.06	0.39 ± 0.06	0.15 ± 0.15	0.30 ± 0.06	0.37 ± 0.06	0.32 ± 0.09	0.43 ± 0.11	0.35 ± 0.02	0.29 ± 0.16	0.48 ± 0.14	0.38 ± 0.04	0.38 ± 0.05	0.30 ± 0.02
Chlorogenic acid derivative 6	-	-	-	-	-	-	-	-	0.04 ± 0.04	0.29 ± 0.29	0.12 ± 0.09	-	0.44 ± 0.04	0.36 ± 0.05	0.51 ± 0.02	0.52 ± 0.13
Sum, phenolic acids	*9.48 ± 2.85*	*8.24 ± 1.95*	*7.20 ± 1.39*	*8.95 ± 2.93*	*15.89 ± 3.67*	*15.71 ± 14.06*	*11.52 ± 4.62*	*16.17 ± 4.19*	*5.25 ± 0.45*	*5.34 ± 1.70*	*6.17 ± 0.81*	*6.35 ± 1.18*	*6.74 ± 0.62*	*6.21 ± 1.12*	*8.53 ± 1.19*	*6.98 ± 1.07*
OTHERS																
Sum, low molecular phenolics	*64.83 ± 3.31*	*60.31 ± 7.92*	*65.96 ± 7.44*	*69.31 ± 11.09*	*66.05 ± 4.79*	*57.37 ± 29.37*	*59.54 ± 9.67*	*60.06 ± 21.61*	*74.78 ± 8.51*	*63.54 ± 10.51*	*63.59 ± 8.03*	*88.63 ± 14.98*	*95.21 ± 10.15*	*63.17 ± 4.62*	*85.11 ± 18.96*	*78.51 ± 13.55*
CONDENSED TANNINS																
MeOH soluble	32.89 ± 0.25	28.74 ± 2.07	24.33 ± 1.82	19.65 ± 1.83	24.84 ± 2.39	12.67 ± 3.79	19.41 ± 2.47	22.50 ± 3.30	35.64 ± 2.16	35.53 ± 8.91	27.76 ± 2.49	22.46 ± 0.82	31.32 ± 1.93	43.29 ± 4.40	28.00 ± 0.61	26.84 ± 4.31
MeOH insoluble	100.72 ± 70.20	50.76 ± 14.80	35.60 ± 4.67	23.57 ± 1.92	30.22 ± 7.34	39.37 ± 12.41	22.77 ± 2.51	56.57 ± 16.09	203.37 ± 179.01	31.71 ± 11.49	39.07 ± 6.59	32.31 ± 6.34	13.40 ± 4.69	20.76 ± 2.66	19.87 ± 4.26	28.24 ± 6.33
Sum, condensed tannins	*133.61 ± 70.45*	*79.50 ± 12.73*	*59.93 ± 5.86*	*43.22 ± 2.68*	*55.06 ± 8.78*	*52.04 ± 16.21*	*42.18 ± 1.59*	*79.07 ± 15.30*	*239.02 ± 178.50*	*67.25 ± 20.16*	*66.82 ± 7.24*	*54.76 ± 5.55*	*44.72 ± 4.52*	*64.05 ± 6.39*	*47.88 ± 3.71*	*55.08 ± 9.35*

Betula pendula	**Green leaves**	**Yellow leaves**

	Dark	No-UVA/Blue	No-UVA	Full-spectrum	Dark	No-UVA/Blue	No-UVA	Full-spectrum
FLAVONOIDS								
Quercetin glycoside 1	9.71 ± 0.99	13.30 ± 1.87	7.87 ± 0.94	13.28 ± 3.21	7.04 ± 0.92	7.80 ± 1.25	7.75 ± 0.83	5.23 ± 0.84
Quercetin glycoside 2	1.92 ± 0.80	3.18 ± 0.72	0.85 ± 0.40	1.74 ± 0.63	2.11 ± 0.43	3.01 ± 0.45	2.29 ± 0.56	1.51 ± 0.35
Quercetin glycoside 3	1.07 ± 0.19	0.83 ± 0.16	0.81 ± 0.15	0.79 ± 0.24	0.49 ± 0.10	0.53 ± 0.14	0.57 ± 0.11	0.70 ± 0.12
Quercetin glycoside 4	0.22 ± 0.17	0.87 ± 0.30	0.18 ± 0.14	0.93 ± 0.45	1.69 ± 0.34	1.37 ± 0.20	1.20 ± 0.13	1.02 ± 0.20
Quercetin glycoside 5	3.22 ± 1.11	4.94 ± 0.90	2.93 ± 1.11	4.08 ± 1.33	2.43 ± 0.95	2.19 ± 0.96	1.34 ± 0.47	1.47 ± 0.27
Quercetin glycoside 6	26.03 ± 1.83	28.09 ± 2.44	25.01 ± 2.58	25.93 ± 3.57	21.40 ± 1.52	21.64 ± 2.57	24.05 ± 3.06	23.03 ± 3.53
Quercetin glycoside 7	8.46 ± 1.44	9.19 ± 1.09	6.33 ± 1.71	7.01 ± 1.44	7.53 ± 0.71	8.36 ± 0.80	8.58 ± 0.92	7.54 ± 1.46
Quercetin glycoside 8	0.64 ± 0.12	0.76 ± 0.24	0.58 ± 0.14	0.64 ± 0.21	1.96 ± 0.65	2.78 ± 0.83	1.02 ± 0.26	2.45 ± 0.64
Quercetin glycoside 9	6.04 ± 0.47	6.94 ± 0.73	6.02 ± 0.72	6.30 ± 0.87	4.62 ± 0.62	3.23 ± 0.77	5.44 ± 0.56	4.50 ± 1.24
Quercetin aglycon	1.09 ± 0.36	0.76 ± 0.14	0.72 ± 0.06	0.77 ± 0.05	0.85 ± 0.20	0.83 ± 0.20	0.61 ± 0.14	0.53 ± 0.13
Apigenin glycoside 1	2.14 ± 0.56	2.41 ± 0.35	2.18 ± 0.42	1.88 ± 0.27	1.22 ± 0.37	1.28 ± 0.30	1.14 ± 0.51	1.59 ± 0.25
Apigenin glycoside 2	0.72 ± 0.16	0.87 ± 0.12	0.92 ± 0.33	0.73 ± 0.16	0.67 ± 0.23	1.01 ± 0.37	0.66 ± 0.21	0.86 ± 0.40
Sum, flavonoids	*61.10 ± 4.34*	*72.30 ± 5.24*	*54.40 ± 3.33*	*63.98 ± 8.56*	*51.71 ± 2.28*	*53.83 ± 4.76*	*54.67 ± 5.33*	*50.77 ± 6.45*
PHENOLIC ACIDS								
Hydroxycinnamic acid (HCA)	0.57 ± 0.16	0.59 ± 0.14	0.53 ± 0.13	0.39 ± 0.14	0.40 ± 0.09	0.61 ± 0.12	0.42 ± 0.09	0.64 ± 0.13
Neochlorogenic acid	12.86 ± 4.18	10.99 ± 3.10	9.38 ± 2.01	8.68 ± 0.94	14.68 ± 3.01	19.57 ± 4.36	17.21 ± 4.31	16.13 ± 2.12
Chlorogenic acid	0.50 ± 0.13	0.77 ± 0.15	1.34 ± 0.62	1.11 ± 0.32	0.69 ± 0.07	0.59 ± 0.17	0.77 ± 0.16	0.68 ± 0.26
Sum, phenolic acids	*13.80 ± 4.28*	*12.30 ± 3.00*	*10.95 ± 1.84*	*10.78 ± 0.99*	*15.94 ± 2.96*	*20.67 ± 4.37*	*18.54 ± 4.22*	*17.12 ± 2.13*
OTHERS								
Sum, low molecular phenolics	*74.91 ± 4.66*	*84.60 ± 6.08*	*65.35 ± 3.72*	*74.76 ± 8.10*	*67.65 ± 3.73*	*74.50 ± 8.24*	*73.21 ± 8.32*	*67.88 ± 6.15*
CONDENSED TANNINS								
MeOH soluble	2.42 ± 0.42	2.42 ± 0.36	3.22 ± 1.08	2.75 ± 0.47	7.33 ± 1.02	11.54 ± 2.40	6.13 ± 1.45	9.98 ± 2.94
MeOH insoluble	17.95 ± 1.92	19.02 ± 2.74	21.64 ± 3.52	22.16 ± 2.69	18.26 ± 3.40	14.61 ± 1.08	19.45 ± 1.46	15.39 ± 2.37

Sum, condensed tannins	*20.37 ± 2.32*	*21.44 ± 2.74*	*24.87 ± 4.57*	*24.91 ± 2.91*	*25.60 ± 3.51*	*26.15 ± 2.73*	*25.58 ± 2.58*	*25.37 ± 4.76*

Table S7 ANOVA table for the phenolic compounds isolated from leaf litter of *B. pendula* and *F. sylvatica* by HLPC follow the controlled-conditions experiment.

Fagus sylvatica	**Colour (C)**	**Orientation (O)**	**Filter treatment (F)**	**C x O x F**	**C x O**	**C x F**	**O x F**
	$F_{1,47}$ **(*p*)**	$F_{1,47}$ **(*p*)**	$F_{3,47}$ **(*p*)**	$F_{3,47}$ **(*p*)**	$F_{3,47}$ **(*p*)**	$F_{1,47}$ **(*p*)**	$F_{1,47}$ **(*p*)**
STILBENES							
Taxifolin xyloside	3.53 (0.066)	0.02 (0.880)	0.38 (0.766)	1.10 (0.358)	1.72 (0.196)	0.20 (0.897)	0.87 (0.464)
Taxifolin glucoside	**4.61 (0.037)**	0.06 (0.805)	0.16 (0.926)	0.21 (0.888)	1.13 (0.292)	0.59 (0.626)	0.10 (0.959)
Taxifolin aglycon	0.17 (0.682)	1.64 (0.207)	0.81 (0.492)	2.24 (0.097)	0.02 (0.898)	0.29 (0.830)	1.81 (0.159)
Sum, stilbenes	*0.26 (0.613)*	*0.28 (0.601)*	*0.36 (0.780)*	*1.39 (0.257)*	*0.003 (0.954)*	*0.48 (0.699)*	*0.08 (0.969)*
FLAVONOIDS							
Myricetin 3-rhamnoside	**12.38 (< 0.001)**	0.67 (0.418)	2.32 (0.087)	0.24 (0.869)	2.88 (0.096)	0.74 (0.533)	1.69 (0.183)
Quercetin 3-rhamnoside	**13.47 (< 0.001)**	**4.41 (0.041)**	0.46 (0.714)	0.04 (0.988)	3.69 (0.06)	0.42 (0.737)	0.44 (0.726)
Quercetin 3-galactoside	**6.99 (0.011)**	0.17 (0.683)	0.40 (0.756)	0.21 (0.891)	**6.37 (0.015)**	0.29 (0.830)	0.41 (0.743)
Quercetin 3-glucoside	**18.87 (< 0.001)**	**9.78 (0.003)**	0.57 (0.636)	0.03 (0.994)	**8.97 (0.004)**	1.81 (0.159)	2.04 (0.122)
Quercetin 7-glycoside	**5.50 (0.023)**	**5.59 (0.022)**	1.33 (0.275)	1.04 (0.383)	0.55 (0.461)	0.36 (0.781)	1.07 (0.370)
Kaempferol 3-galactoside	2.65 (0.110)	0.78 (0.381)	0.49 (0.693)	0.04 (0.988)	**5.77 (0.020)**	0.43 (0.731)	0.30 (0.822)
Kaemperfol 3-glucoside	0.23 (0.629)	**5.53 (0.023)**	1.32 (0.279)	1.01 (0.395)	0.01 (0.936)	0.43 (0.729)	0.84 (0.481)
Kaempferol 3-arabinoside	**12.86 (< 0.001)**	**7.62 (0.008)**	1.69 (0.182)	0.08 (0.972)	**4.21 (0.046)**	0.77 (0.519)	1.05 (0.381)
Kaempferol 3-rhamnoside	2.31 (0.135)	**6.80 (0.012)**	**2.88 (0.046)**	0.94 (0.426)	**6.03 (0.018)**	0.43 (0.734)	0.97 (0.416)
Monocoumaroylastragallin 1	**18.24 (< 0.001)**	**4.75 (0.034)**	0.76 (0.524)	0.37 (0.772)	**5.14 (0.028)**	0.40 (0.753)	0.43 (0.735)
Monocoumaroylastragallin 2	**10.27 (0.002)**	2.77 (0.102)	0.54 (0.657)	1.80 (0.159)	2.02 (0.161)	0.37 (0.772)	0.57 (0.636)
Monocoumaroylastragallin 3	**50.66 (< 0.001)**	2.76 (0.103)	0.76 (0.512)	1.40 (0.258)	0.03 (0.856)	0.52 (0.672)	0.51 (0.678)
Monocoumaroylastragallin 4	**11.93 (0.001)**	**5.07 (0.029)**	1.03 (0.388)	3.77 (0.017)	1.84 (0.181)	0.05 (0.986)	1.40 (0.255)
Dicoumaroylastragallin 1	**4.14 (0.049)**	0.07 (0.797)	0.86 (0.472)	0.64 (0.592)	0.02 (0.879)	0.23 (0.877)	1.81 (0.165)
Dicoumaroylastragallin 2	**31.47 (< 0.001)**	0.07 (0.800)	0.81 (0.495)	2.45 (0.076)	2.25 (0.141)	0.37 (0.776)	0.49 (0.687)
Sum, flavonoids	***14.61 (< 0.001)***	*0.86 (0.359)*	*1.22 (0.313)*	*0.28 (0.840)*	***5.41 (0.024)***	*0.57 (0.636)*	*0.83 (0.482)*
PHENOLIC ACIDS							
Hydroxycinnamic acid (HCA)	0.31 (0.578)	2.48 (0.122)	1.25 (0.302)	0.06 (0.982)	1.92 (0.172)	1.79 (0.161)	1.11 (0.355)
Neochlorogenic acid	**5.34 (0.025)**	0.96 (0.332)	**3.40 (0.025)**	0.86 (0.469)	0.21 (0.650)	0.62 (0.602)	1.86 (0.149)
Chlorogenic acid	**5.19 (0.027)**	**17.17 (< 0.001)**	0.40 (0.750)	0.31 (0.818)	**9.32 (0.004)**	0.55 (0.652)	0.01 (0.998)
Chlorogenic acid derivative 1	**52.34 (< 0.001)**	2.74 (0.105)	0.28 (0.842)	0.58 (0.628)	**15.12 (< 0.001)**	2.49 (0.072)	0.90 (0.447)
Chlorogenic acid derivative 2	**41.32 (< 0.001)**	0.59 (0.448)	0.46 (0.709)	0.38 (0.765)	1.77 (0.190)	0.47 (0.705)	0.51 (0.675)
Chlorogenic acid derivative 3	**32.02 (< 0.001)**	0.06 (0.809)	0.16 (0.923)	0.56 (0.641)	3.44 (0.070)	1.66 (0.188)	0.26 (0.853)

Chlorogenic acid derivative 4	1.39 (0.255)	3.60 (0.066)	0.75 (0.530)	2.33 (0.111)	3.44 (0.071)	0.15 (0.997)	0.83 (0.485)
Chlorogenic acid derivative 5	**5.74 (0.021)**	0.47 (0.497)	2.07 (0.117)	1.93 (0.139)	1.65 (0.206)	0.14 (0.936)	0.06 (0.980)
Chlorogenic acid derivative 6	**80.11 (< 0.001)**	**25.22 (< 0.001)**	1.21 (0.317)	0.64 (0.595)	**29.83 (< 0.001)**	0.26 (0.850)	0.78 (0.513)
Sum, phenolic acids	***9.78 (0.003)***	***6.69 (0.013)***	*0.42 (0.740)*	*0.16 (0.923)*	*1.21 (0.276)*	*0.64 (0.592)*	*0.08 (0.969)*
OTHERS							
Sum, low molecular phenolics	***4.79 (0.034)***	*0.01 (0.912)*	*1.21 (0.317)*	*0.30 (0.824)*	*2.00 (0.164)*	*0.20 (0.892)*	*0.55 (0.647)*
CONDENSED TANNINS							
MeOH soluble	**20.39 (< 0.001)**	2.20 (0.144)	**5.52 (0.002)**	2.41 (0.078)	**4.54 (0.038)**	**2.81 (0.049)**	0.92 (0.489)
MeOH insoluble	0.29 (0.595)	2.60 (0.113)	0.92 (0.439)	0.15 (0.928)	0.73 (0.397)	0.12 (0.945)	1.68 (0.185)
Sum, condensed tannins	*0.22 (0.643)*	*3.97 (0.052)*	*1.01 (0.398)*	*0.30 (0.825)*	*0.11 (0.743)*	*0.05 (0.983)*	*2.36 (0.084)*

Betula pendula	**Colour (C)** $F_{1,55}$ **(*p*)**	**Filter treatment (F)** $F_{3,55}$ **(*p*)**	**C x F** $F_{1,55}$ **(*p*)**
FLAVONOIDS			
Quercetin glycoside 1	**16.71 (< 0.001)**	1.60 (0.199)	2.48 (0.070)
Quercetin glycoside 2	2.98 (0.092)	2.68 (0.060)	2.43 (0.079)
Quercetin glycoside 3	**4.68 (0.035)**	0.15 (0.929)	0.44 (0.721)
Quercetin glycoside 4	0.88 (0.353)	0.41 (0.745)	1.85 (0.154)
Quercetin glycoside 5	**10.98 (0.002)**	0.88 (0.458)	0.83 (0.483)
Quercetin glycoside 6	**4.17 (0.046)**	0.10 (0.957)	0.28 (0.837)
Quercetin glycoside 7	0.27 (0.608)	0.79 (0.504)	0.74 (0.529)
Quercetin glycoside 8	**23.69 (< 0.001)**	1.56 (0.209)	0.89 (0.454)
Quercetin glycoside 9	**13.24 (< 0.001)**	0.32 (0.808)	1.50 (0.224)
Quercetin aglycon	0.27 (0.608)	1.27 (0.294)	0.15 (0.923)
Apigenin glycoside 1	**11.30 (0.001)**	0.80 (0.500)	0.69 (0.561)
Apigenin glycoside 2	0.37 (0.542)	0.47 (0.705)	0.36 (0.779)
Sum, flavonoids	***7.18 (0.010)***	*1.19 (0.322)*	*0.85 (0.473)*
PHENOLIC ACIDS			
Hydroxycinnamic acid (HCA)	0.01 (0.929)	0.28 (0.837)	0.72 (0.544)
Neochlorogenic acid	**8.37 (0.005)**	0.03 (0.992)	0.36 (0.779)
Chlorogenic acid	2.78 (0.102)	**2.80 (0.050)**	1.88 (0.147)
Sum, phenolic acids	***7.61 (0.008)***	*0.02 (0.995)*	*0.25 (0.862)*
OTHERS			

Sum, low molecular phenolics	*1.03 (0.315)*	*1.01 (0.394)*	*0.61 (0.611)*
CONDENSED TANNINS			
MeOH soluble	**48.88 (< 0.001)**	0.44 (0.721)	1.59 (0.203)
MeOH insoluble	3.59 (0.063)	0.67 (0.573)	0.35 (0.790)
Sum, condensed tannins	***6.05 (0.017)***	*0.29 (0.830)*	*0.32 (0.810)*

Table S8 Pairwise comparisons for HPLC phenolics responding to filter treatments in *Fagus sylvatica* leaves in the controlled experiment: t- tests, with the Holm's correction for multiple comparisons, were used to calculate the P values. Significant contrasts are shown in bold.

Kaempferol 3-rhamnoside				
Filter	**Estimate**	**SE**	**t-value**	**P value**
Dark - No-UVA/Blue	0.237	0.098	2.426	0.074
Dark - No-UVA	-0.019	0.091	-0.211	1.000
Dark - Full-Spectrum	-0.041	0.095	-0.432	1.000
No-UVA/Blue - No-UVA	**-0.256**	**0.094**	**-2.729**	**0.042**
No-UVA/Blue - Full-Spectrum	**-0.278**	**0.098**	**-2.843**	**0.037**
No-UVA - Full-Spectrum	-0.022	0.092	-0.237	1.000
Neochlorogenic acid				
Filter	**Estimate**	**SE**	**t-value**	**P value**
Dark - No-UVA/Blue	-0.102	0.079	-1.291	0.617
Dark - No-UVA	-0.185	0.074	-2.509	0.076
Dark - Full-Spectrum	**-0.218**	**0.078**	**-2.806**	**0.042**
No-UVA/Blue - No-UVA	-0.084	0.078	-1.087	0.617
No-UVA/Blue - Full-Spectrum	-0.116	0.080	-1.445	0.617
No-UVA - Full-Spectrum	-0.033	0.076	-0.431	0.668
MeOH soluble condensed tannins				
Green leaves				
Filter	**Estimate**	**SE**	**t-value**	**P value**
Dark - No-UVA/Blue	0.912	0.387	2.354	0.411
Dark - No-UVA	0.702	0.336	2.088	0.633
Dark - Full-Spectrum	0.783	0.364	2.152	0.585
No-UVA/Blue - No-UVA	-0.210	0.349	-0.601	1.000
No-UVA/Blue - Full-Spectrum	-0.129	0.376	-0.343	1.000
No-UVA - Full-Spectrum	0.081	0.323	0.251	1.000
Yellow leaves				
Filter	**Estimate**	**SE**	**t-value**	**P value**
Dark - No-UVA/Blue	-0.421	0.331	-1.272	1.000
Dark - No-UVA	0.506	0.336	1.505	1.000
Dark - Full-Spectrum	0.855	0.336	2.544	0.286
No-UVA/Blue - No-UVA	0.926	0.331	2.801	0.155
No-UVA/Blue - Full-Spectrum	**1.276**	**0.331**	**3.857**	**0.009**
No-UVA - Full-Spectrum	0.349	0.336	1.039	1.000

Table S9 Pairwise comparisons for HPLC phenolics responding to filter treatments in *Betula pendula* leaves in the controlled experiment: t- tests, with the Holm's correction for multiple comparisons, were used to calculate the P values. Significant contrasts are shown in bold.

Chlorogenic acid				
Filter	**Estimate**	**SE**	**t-value**	**P value**
Dark - No-UVA/Blue	-0.028	0.104	-0.265	0.792
Dark - No-UVA	**-0.345**	**0.117**	**-2.956**	**0.029**
Dark - Full-Spectrum	-0.212	0.113	-1.875	0.268
No-UVA/Blue - No-UVA	**-0.317**	**0.112**	**-2.823**	**0.035**
No-UVA/Blue - Full-Spectrum	-0.184	0.108	-1.697	0.289
No-UVA - Full-Spectrum	0.133	0.120	1.106	0.549

Table S10 List of pairwise comparisons between forest stands for daily mass loss of green and yellow leaves of *Fagus sylvatica* and *Betula pendula* in the forest experiment: t- tests, with the Holm's correction for multiple comparisons, were used to calculate the P values. Significant contrasts are shown in bold.

Fagus sylvatica – green leaves

	Estimate	Sigma	t-value	p-value
Picea abies - Fagus sylvatica	0.002953929	0.005056817	0.5841479	5.607852e-01
Picea abies - Acer platanoides	**0.025573700**	**0.005056817**	**5.0572721**	**2.697791e-06**
Picea abies - Betula pendula	**0.035232408**	**0.005056817**	**6.9673092**	**8.629000e-10**
Fagus sylvatica - Acer platanoides	**0.022619771**	**0.005056817**	**4.4731242**	**2.552844e-05**
Fagus sylvatica - Betula pendula	**0.032278479**	**0.005056817**	**6.3831613**	**1.099344e-08**
Acer platanoides - Betula pendula	0.009658708	0.005056817	1.9100371	5.975779e-02

Fagus sylvatica – yellow leaves

	Estimate	Sigma	t-value	p-value
Picea abies - Fagus sylvatica	-0.004850646	0.002870346	-1.6899166	0.095037167
Picea abies - Acer platanoides	**-0.008397483**	**0.002906365**	**-2.8893419**	**0.004996198**
Picea abies - Betula pendula	**-0.005945492**	**0.002870346**	**-2.0713500**	**0.041632619**
Fagus sylvatica - Acer platanoides	-0.003546837	0.002906365	-1.2203687	0.226001819
Fagus sylvatica - Betula pendula	-0.001094846	0.002870346	-0.3814334	0.703918777
Acer platanoides - Betula pendula	0.002451991	0.002906365	0.8436625	0.401437997

Betula pendula – green leaves

	Estimate	Sigma	t-value	p-value
Picea abies - Fagus sylvatica	**0.083368627**	**0.01927312**	**4.3256428**	**4.951291e-05**
Picea abies - Acer platanoides	**0.150936050**	**0.01847946**	**8.1677740**	**8.967271e-12**
Picea abies - Betula pendula	**0.089233679**	**0.02036276**	**4.3821992**	**4.042020e-05**
Fagus sylvatica - Acer platanoides	**0.067567423**	**0.01927312**	**3.5057857**	**7.989121e-04**
Fagus sylvatica - Betula pendula	0.005865052	0.02109605	0.2780166	7.818192e-01
Acer platanoides - Betula pendula	**-0.061702371**	**0.02036276**	**-3.0301572**	**3.423368e-03**

Betula pendula – yellow leaves

	Estimate	Sigma	t-value	p-value
Picea abies - Fagus sylvatica	**0.0497523513**	**0.009251949**	**5.37749939**	**8.036199e-07**
Picea abies - Acer platanoides	**0.0426155583**	**0.009024600**	**4.72215487**	**1.044825e-05**
Picea abies - Betula pendula	**0.0504409127**	**0.009137846**	**5.52000008**	**4.519126e-07**
Fagus sylvatica - Acer platanoides	-0.0071367930	0.009251949	-0.77138264	4.428719e-01
Fagus sylvatica - Betula pendula	0.0006885613	0.009366877	0.07351023	9.415932e-01
Acer platanoides - Betula pendula	0.0078253543	0.009137846	0.85636747	3.944867e-01

Description of understorey light estimation

Above canopy PAR

Above canopy PAR was obtained from the Viikki Fields Weather Station of the University of Helsinki located within the experimental site (60°13'39.7'N, 25°01'09.5'E). Additionally, PAR was measured at regular intervals during the experiments in all the forest stands and in a nearby open area using an array spectroradiometer (Maya2000 Pro Ocean Optics, Dunedin, FL, USA; D7-H-SMA cosine diffuser, Bentham Instruments Ltd, Reading, UK) that had been calibrated within the previous 12 months (see Hartikainen et al 2018 for details of the calibration), [39, 40] (Table S1 and S2).

Above canopy UV radiation

Above canopy UV radiation was obtained from the Finnish Meteorological Institute (FMI) weather station located in the adjacent suburb of Kumpula (60°12'00.0"N, 24°57'36.0"E), Helsinki [43, 44]. Additionally, UV radiation was measured at regular intervals during the experiments in all the forest stands and in a nearby open area using an array spectroradiometer (Maya2000 Pro Ocean Optics, Dunedin, FL, USA; D7-H-SMA cosine diffuser, Bentham Instruments Ltd, Reading, UK) that had been calibrated within the previous 12 months (see Hartikainen et al 2018 for details of the calibration), [39, 40] (Table S1 and S2).

Understorey PAR

Transmission percentages of different PAR wavelengths were calculated through comparisons of measurements made in the understorey of each forest stand with measurements in the open area nearby as mentioned above. Hemispherical photos were taken at the same locations as spectral irradiance, to characterize canopy cover of each stand by calculation of the global light index (GLI) through the software Hemisfer, as defined by [41, 42]. The GLI was calculated over several dates during the experiment (once every 15 days) in order to account for sun elevation angle and sunrise and sunset time. GLI were estimated for both clear sky and totally overcast conditions. Several GLI indexes have been used to calculate the amount of the above canopy PAR transmitted through the understorey over the study period taking into account the cloudiness per each day. Days have been considered cloudy when the diffuse radiation was higher than 30% of direct radiation. An average GLI has been employed for partially cloudy days. The understorey PAR was then corrected per wavelength using the transmission percentages calculated from the measurements taken with the Maya spectroradiometer. This allowed us to also estimate the amount of blue light in the understorey.

Understorey UV radiation

Transmission percentages of different biological spectral weighting functions for UV exposure and unweighted UV radiation were calculated through comparisons of measurements made in the understorey of each forest stand with measurements in the open area nearby as mentioned above,

as well as UV:PAR ratios. These percentages and the UV:PAR ratio in the understorey were used to correct the estimated percentage of transmitted PAR, in order to obtain an index of UV transmittance (GLI_{UV}) for clear and overcast conditions through the period of the experiment, accounting for sun elevation angle and sunrise and sunset time. The several estimated GLI_{uv} for each period of the experiment where used to calculate the understorey UV as a percentage of the above canopy UV obtained from the Kumpula weather station.